

Stratosphere – troposphere Interactions:

Lessons from simplified models

Alan Plumb

MIT

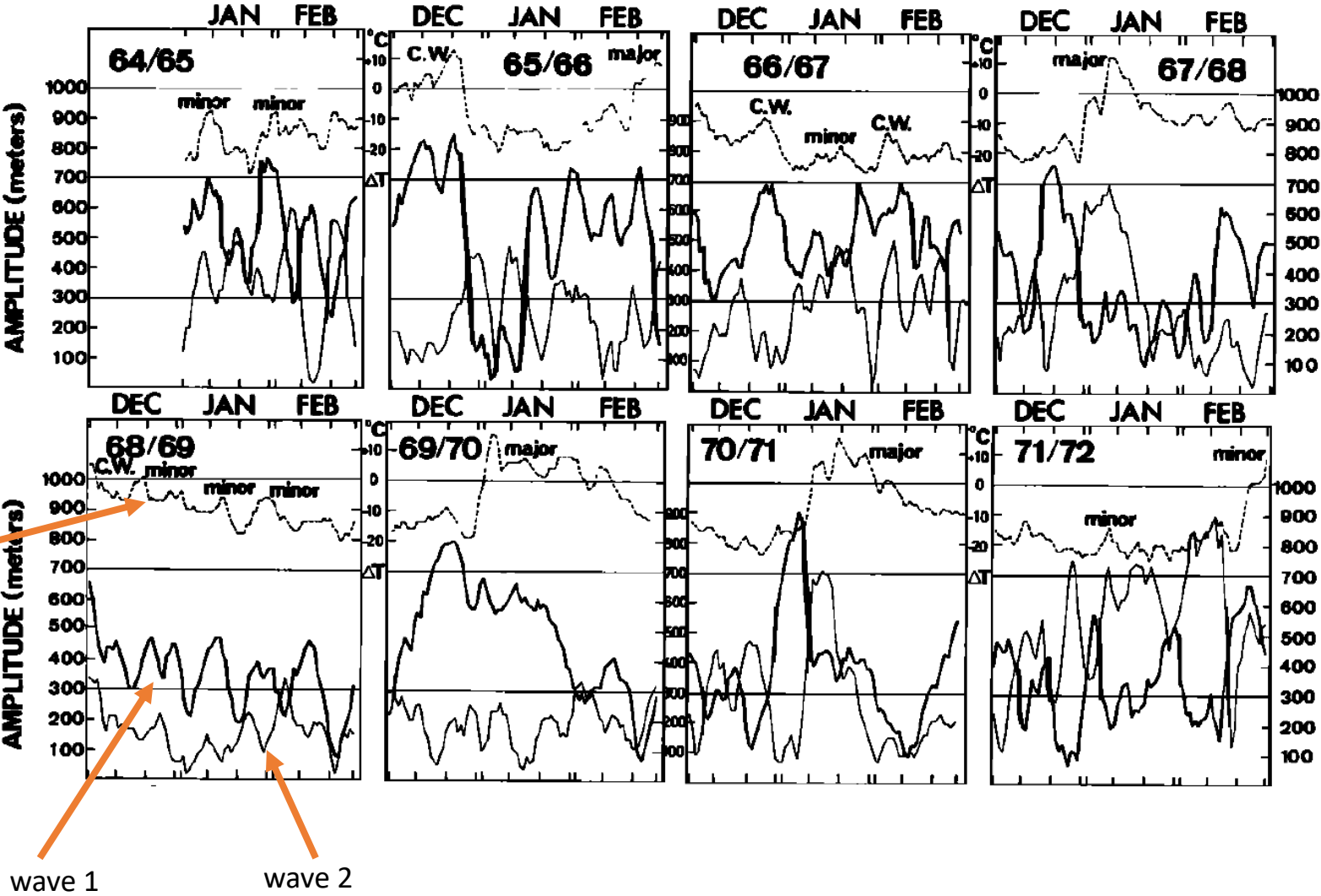
Troposphere



Stratosphere

30hPa

$T_{80} - T_{50}$



Quasi-linear wave, mean flow interaction model
Truncated to single zonal wavenumber

$$\left(\frac{\partial}{\partial t} + im\bar{\omega}\right)\mathcal{L}_m(\psi) + \frac{\partial \bar{q}}{\partial \theta} \frac{im}{\sin^2 \theta \cos \theta} \psi = 0, \quad (14)$$

$$\frac{\partial}{\partial t} \mathcal{L}_0(\bar{\psi}) + \frac{m}{4\Omega a^2} \frac{1}{\cos \theta} \frac{\partial}{\partial \theta} \left[\frac{1}{\sin \theta} \text{Im}(\psi^* \mathcal{L}_m \psi) \right] = 0, \quad (15)$$

where \mathcal{L}_m is defined as

$$\mathcal{L}_m \equiv \frac{1}{\cos \theta} \frac{\partial}{\partial \theta} \left(\frac{\cos \theta}{\sin^2 \theta} \frac{\partial}{\partial \theta} \right) + l^2 \frac{\partial^2}{\partial z^2} - \frac{m^2}{\sin^2 \theta \cos^2 \theta} - \frac{l^2}{4H^2}, \quad (16)$$

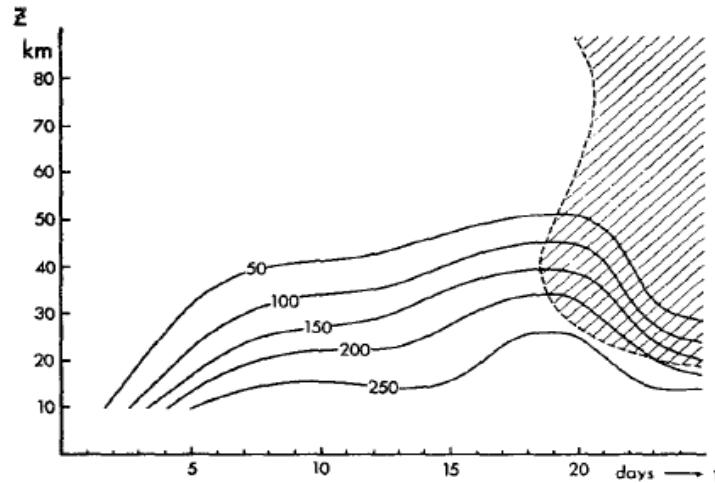


FIG. 12. Time-height section of the wave amplitude at 60N, case C2. Hatched area indicates easterly mean flow.

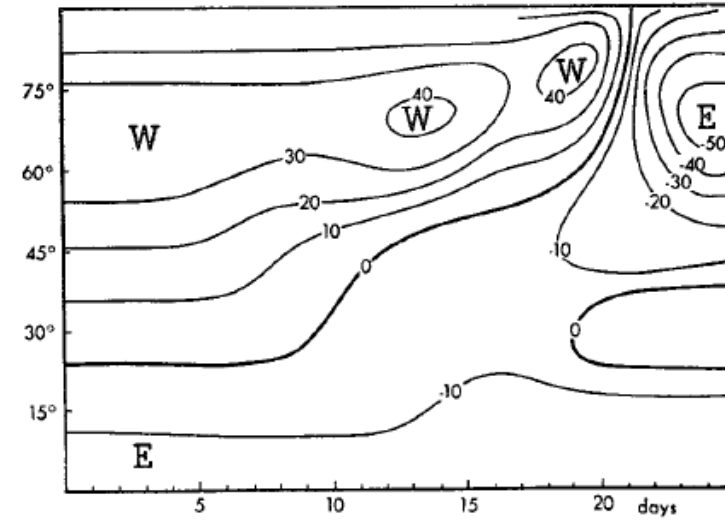
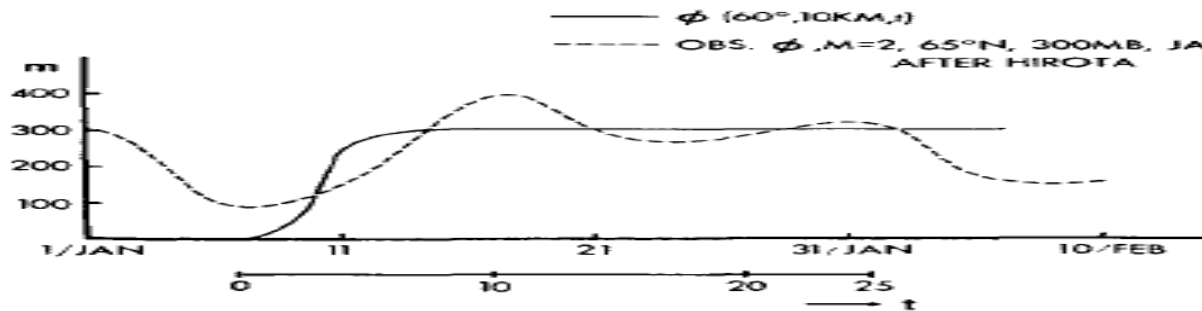


FIG. 17. Time-latitude section of mean zonal winds at $z=30$ km for case C2.

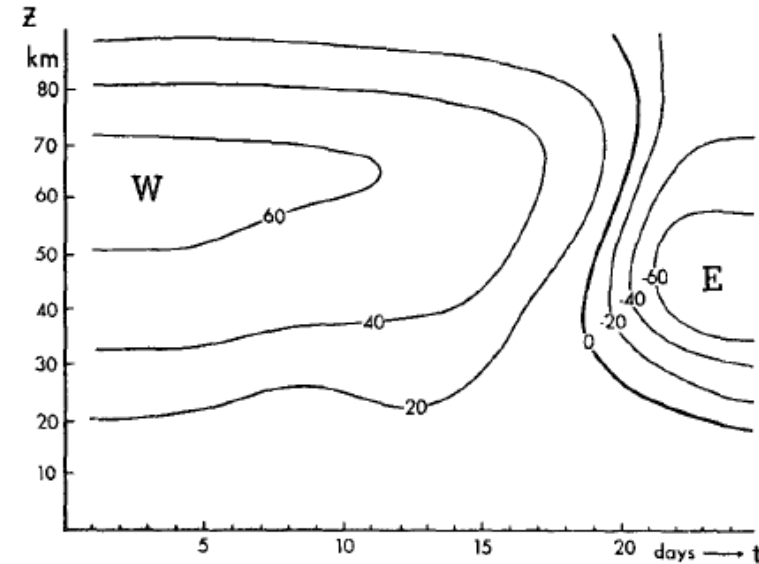


FIG. 13. Same as Fig. 10 except for case C2.

Holton & Mass [1976]

Like Matsuno's model in a beta-channel, but:

- 1) Truncated in latitudinal as well as zonal wavenumber
- 2) Added thermal relaxation to a cold pole state

“not all oscillations in stratospheric long waves can be traced back to oscillations in tropospheric forcing.”

We then impose a geopotential height perturbation at the lower boundary by letting

$$\Psi(z_B, t) = gh(t)/f_0, \quad (11)$$

where $h(t) = h_B[1 - \exp(-t/\tau)]$. Here $\tau = 2.5 \times 10^5$ s

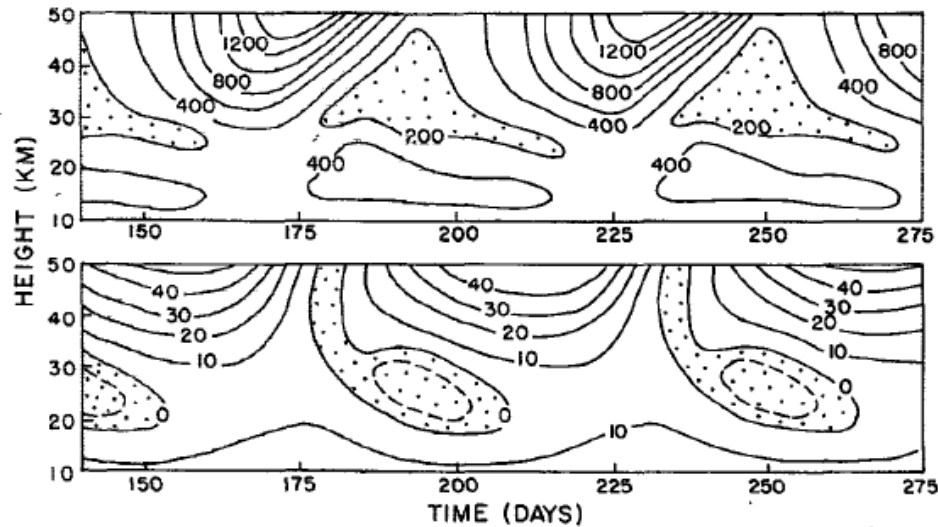


FIG. 7. As in Fig. 6 except for wavenumber 1 forcing with $h_B = 300$ m.

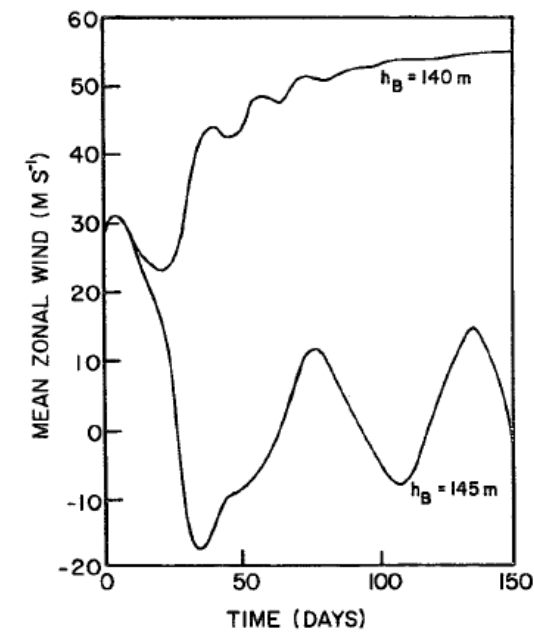


FIG. 2. Time evolutions of the mean zonal wind at 25 km and midchannel for the steady regime ($h_B = 140$ m) and the vacillating regime ($h_B = 145$ m) for zonal wavenumber 2 forcing.

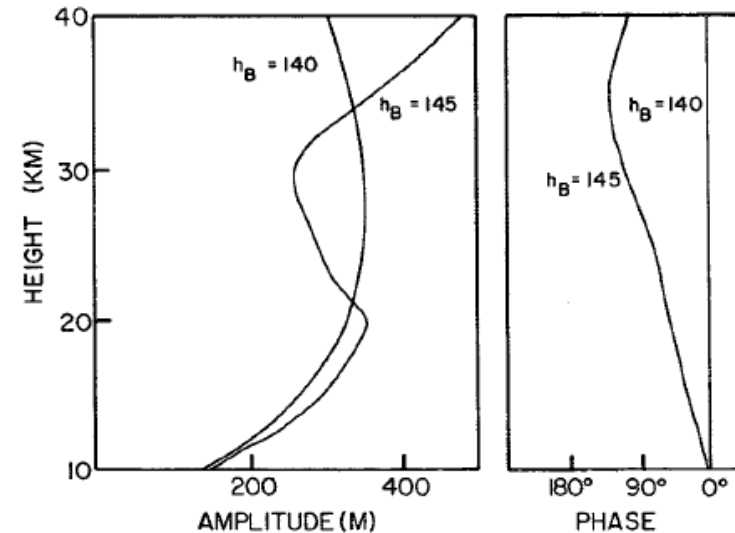


FIG. 3. Vertical profiles of the wave geopotential height perturbation amplitudes and phases averaged in time for day 180 to day 240 for the steady and vacillating regimes with zonal wavenumber 2 forcing.

Plumb [1981]: instability through self-tuned resonance

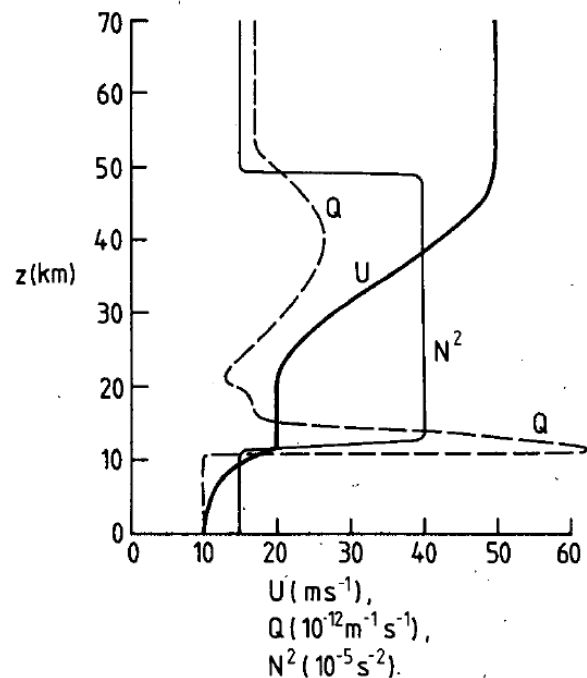


FIG. 3. The vertical structure of the basic state used in this study. Mean zonal wind U , stratification N^2 and potential vorticity gradient Q versus height z .

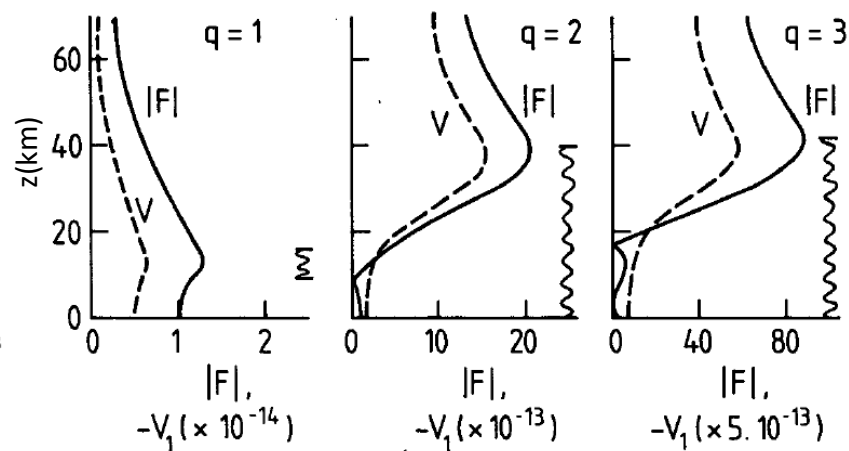


FIG. 4. Structure of the wave amplitude F (solid line) and leading mean flow correction V_1 (dashed line) for the first three modes of wavenumber $(s, m) = (2, 1)$. Other data for these models is given in Table 3. The regions of propagation ($p^2 > 0$) are indicated by the vertical wavy line.

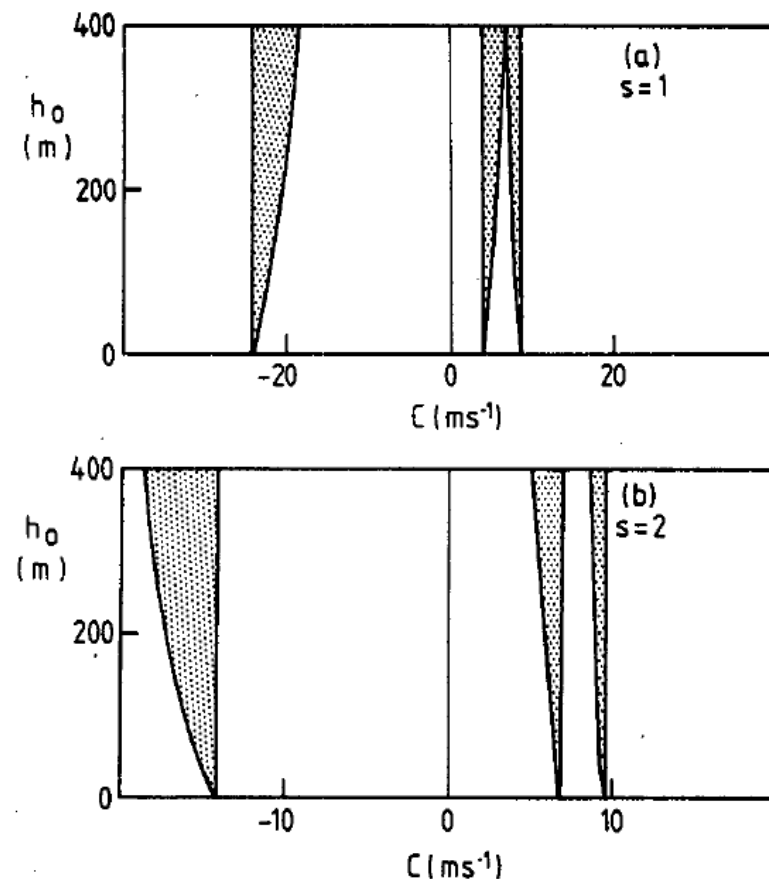


FIG. 5. Instability diagrams for (a) wavenumber $(1, 1)$ and (b) wavenumber $(2, 1)$ associated with the first three modes of each wave. Regions in which the steady wave is unstable to infinitesimal perturbations are shaded.

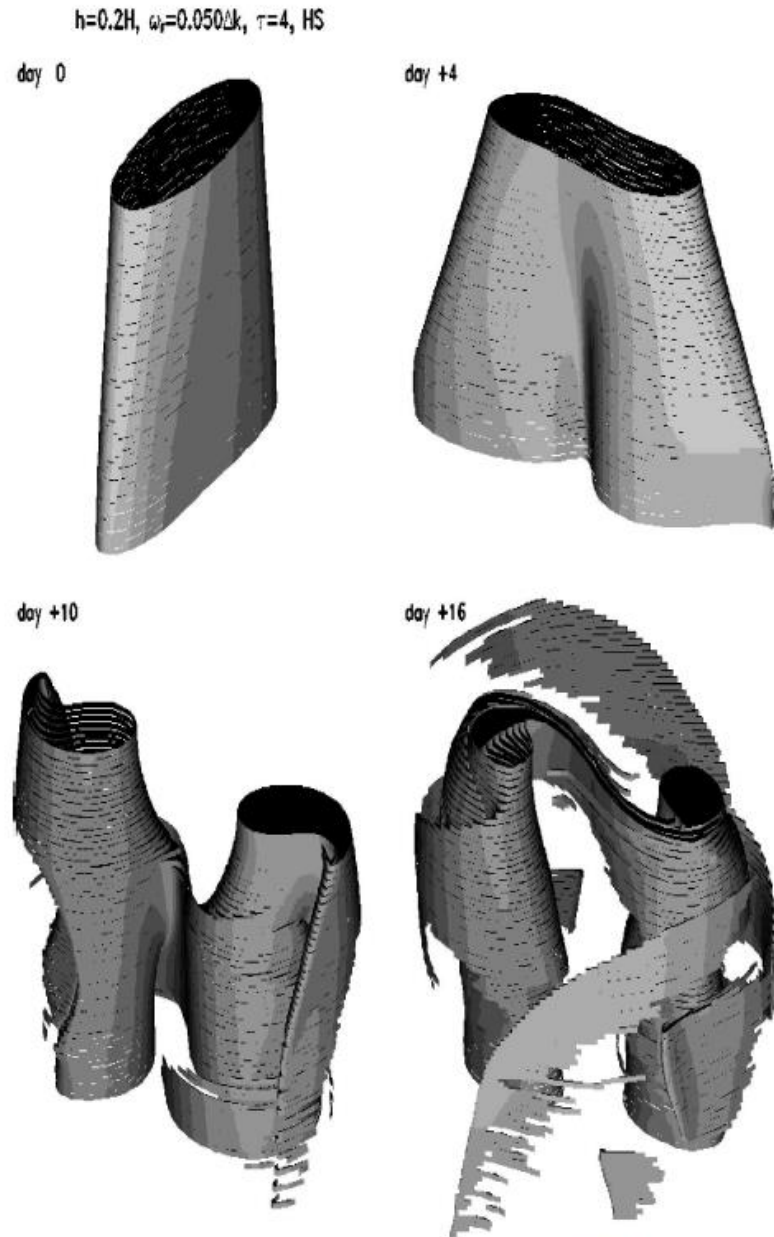


FIG. 9. Surface plots showing the evolution of the vortex during the barotropic sudden warming experiment with $h = 0.2H$, $\tau = 4$ days, HS ($IR = 1.162$) forcing, $\omega_p/\Delta k = 0.05$. The lowest six scale heights ($0 \leq z \leq 6H = 36.84$ km) are shown.

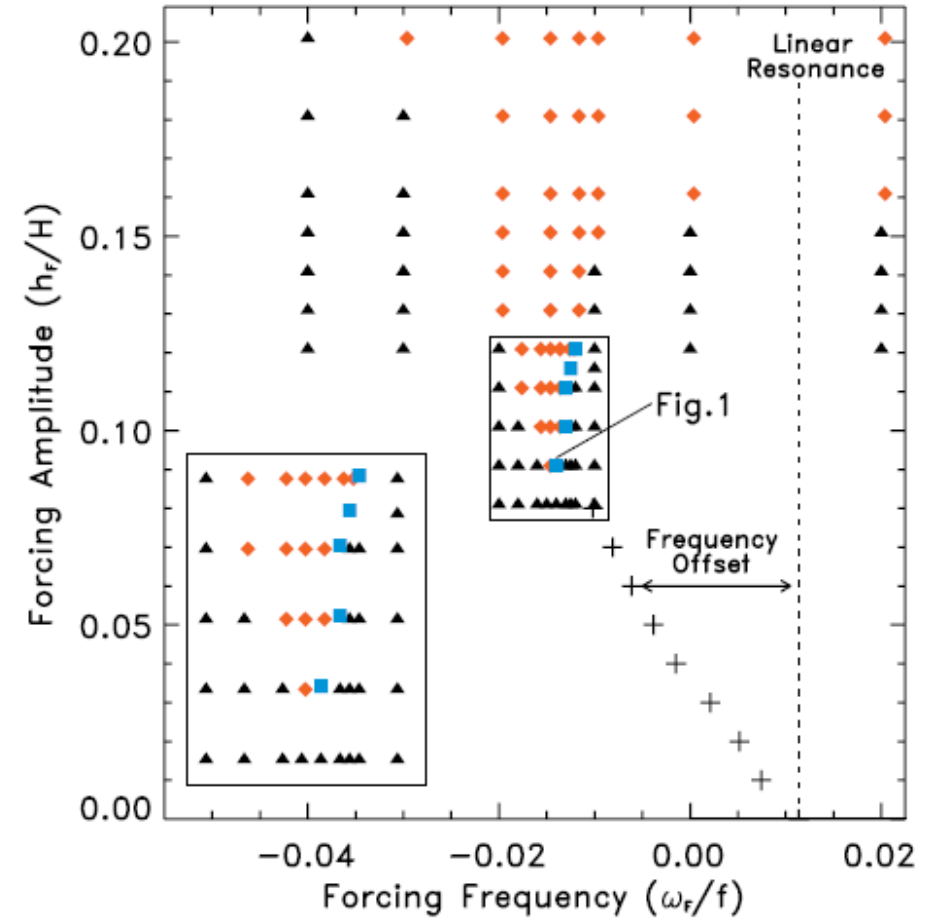


Figure 3. Regime diagram of model behavior as a function of forcing amplitude h_F and forcing frequency ω_F . Red diamonds denote model experiments which result in a complete vortex split, and black triangles denote those experiments in which no split occurs.

Yoden [1987] – bifurcation properties of Holton-Mass model

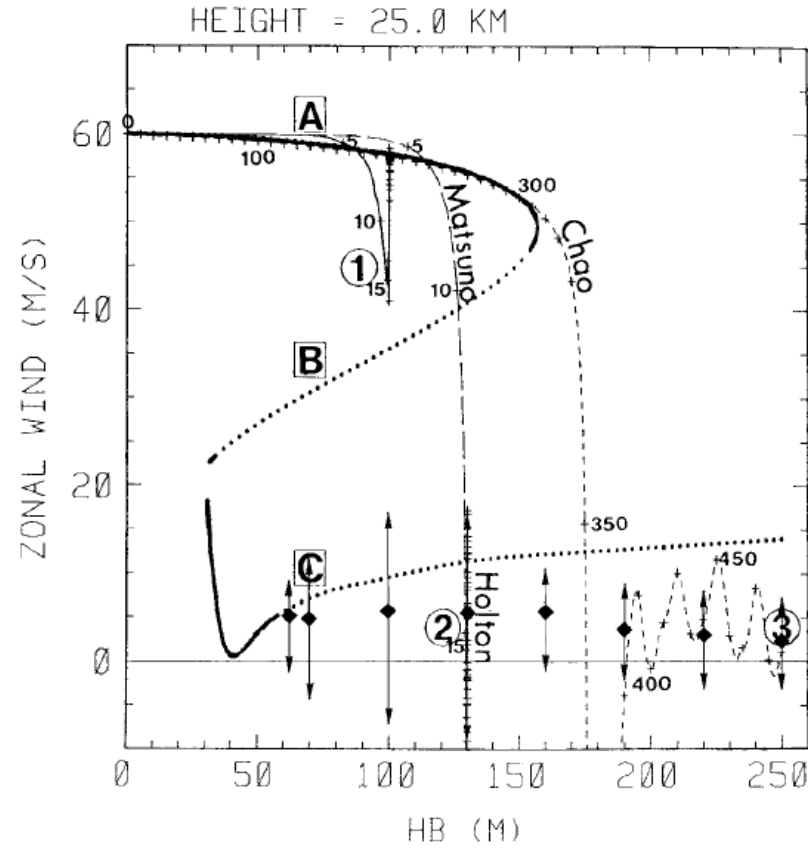


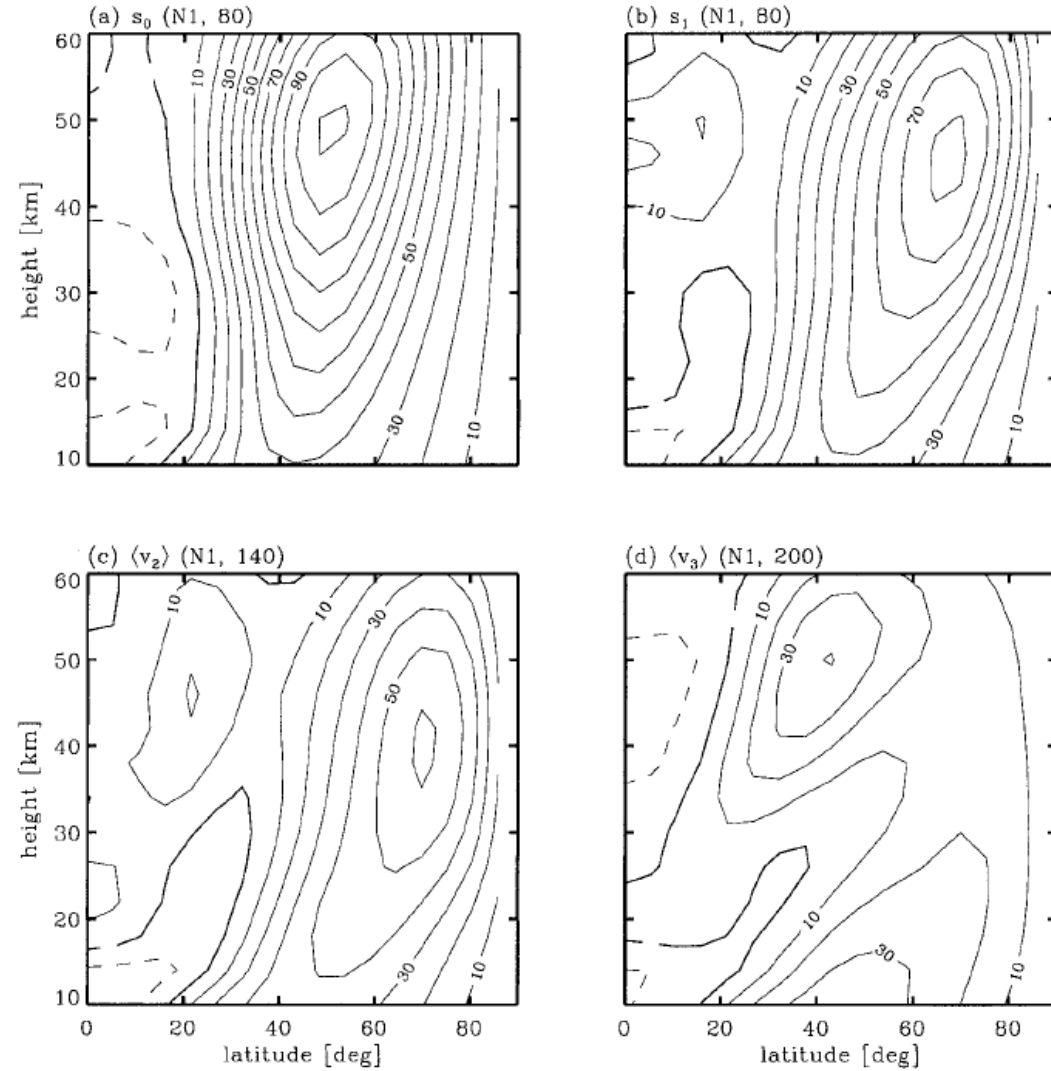
Fig. 5. Bifurcation diagram of the HM model and trajectories of three time-dependent solutions projected onto the same plane; the abscissa is the external parameter h_B and the ordinate is a dependent variable of the model, the mean zonal wind at $z = 25$ km. Steady solution branches (A)–(C) are denoted by solid lines for stable solutions and dotted lines for unstable ones. Variable range of stable vacillations (periodic solutions) are drawn with vertical arrows with two heads, and diamonds denote the time mean values. Three lines (1)–(3) are responses to different wave forcings at the bottom boundary. (1) $h_B = 100 \text{ m} \times [1 - \exp(-t/T)]$ with $T = 2.5 \times 10^5 \text{ s}$, (2) $h_B = 130 \text{ m} \times [1 - \exp(-t/T)]$, (3) $h_B = 0.5 \text{ m day}^{-1} \times t$. Symbol + is put every 5 days for (1) and (2) and 10 days for (3). Unit of label is written in days.

Scott & Haynes [2000] – Zonally truncated stratospheric SGCM has multiple states

2 steady states with same boundary conditions



t-averages of 2 vacillating states



Also Christiansen [1999,2000]

FIG. 1. Height-latitude cross section of zonal mean zonal velocity for two steady-state and two vacillation regimes obtained with radiative basic state N1, corresponding to late Nov, for various wave-forcing amplitudes, h_0 : (a) steady state s_0 , $h_0 = 80$ m; (b) steady state s_1 , $h_0 = 80$ m; (c) vacillation v_2 , $h_0 = 140$ m; (d) vacillation v_3 , $h_0 = 200$ m. Note that (a) and (b) are obtained under identical external (forcing) conditions, but that the approach to steady state is along different solution branches. Also note that (c) and (d) have been averaged over several vacillation cycles. Contour interval is 10 m s^{-1} , solid lines are positive, dashed lines are negative, and thick lines are zero.

Scott & Polvani [2004] – SGCM with inactive troposphere and specified thermal wave forcing in troposphere: sustained wind vacillations and EP flux surges through tropopause

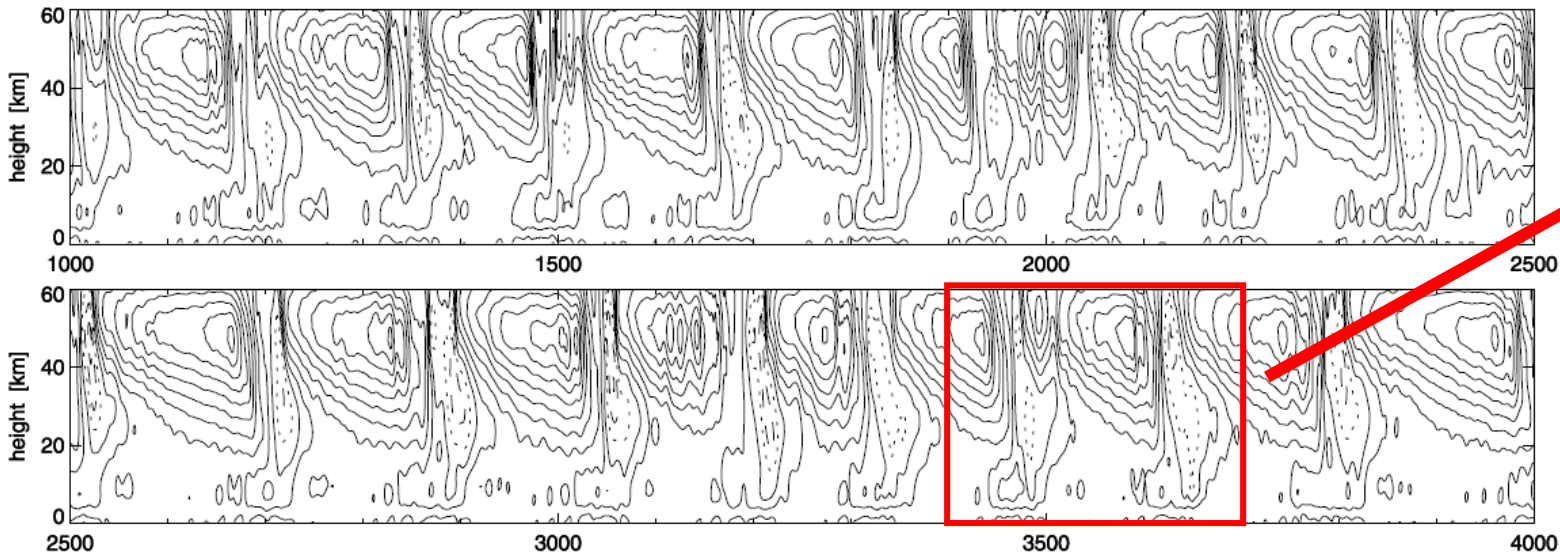


Figure 1. Zonal mean zonal velocity at 60°N as a function of height (in km) and time (in days). Numerical resolution is T42, with 40 vertical levels. The tropospheric wave forcing amplitude $A = 2 \times 10^{-4} \text{ K s}^{-1}$, and the radiative equilibrium vortex strength $\gamma = 2$. The contour interval is 10 ms^{-1} , with positive, negative, and zero values shown solid, dashed, and dotted, respectively.

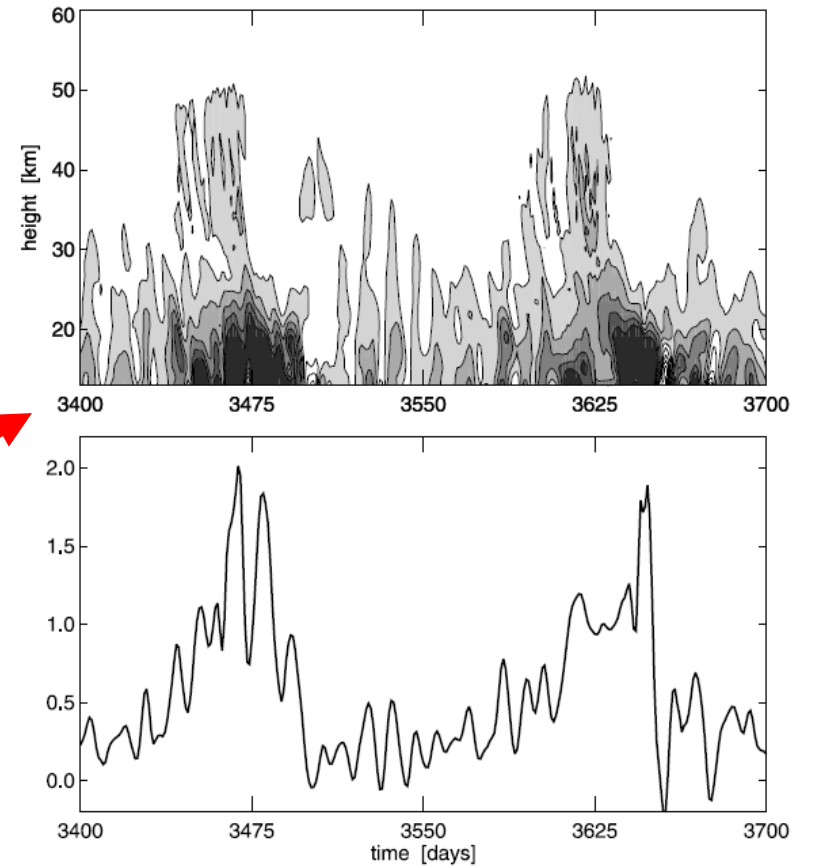
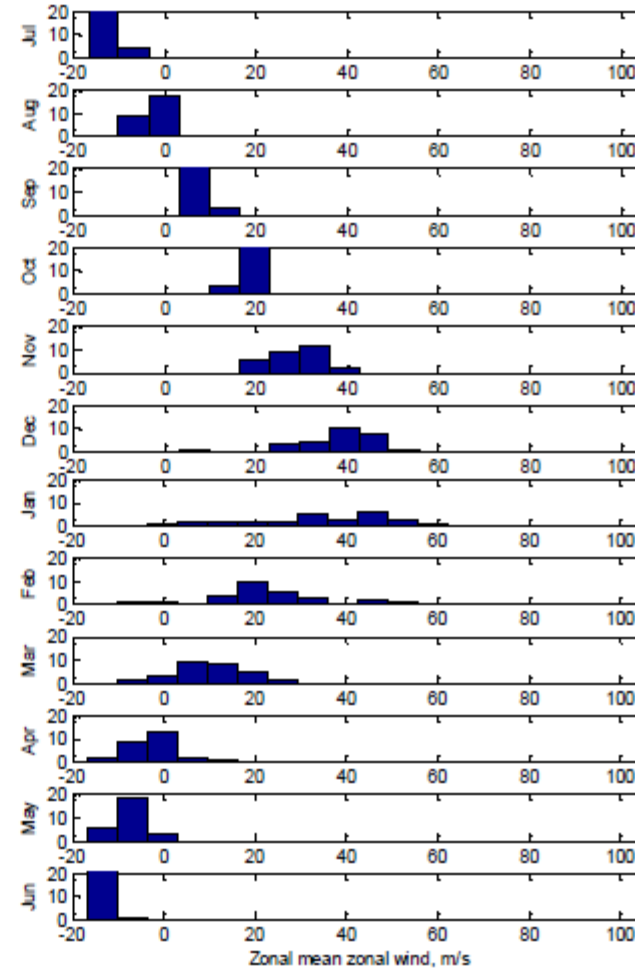
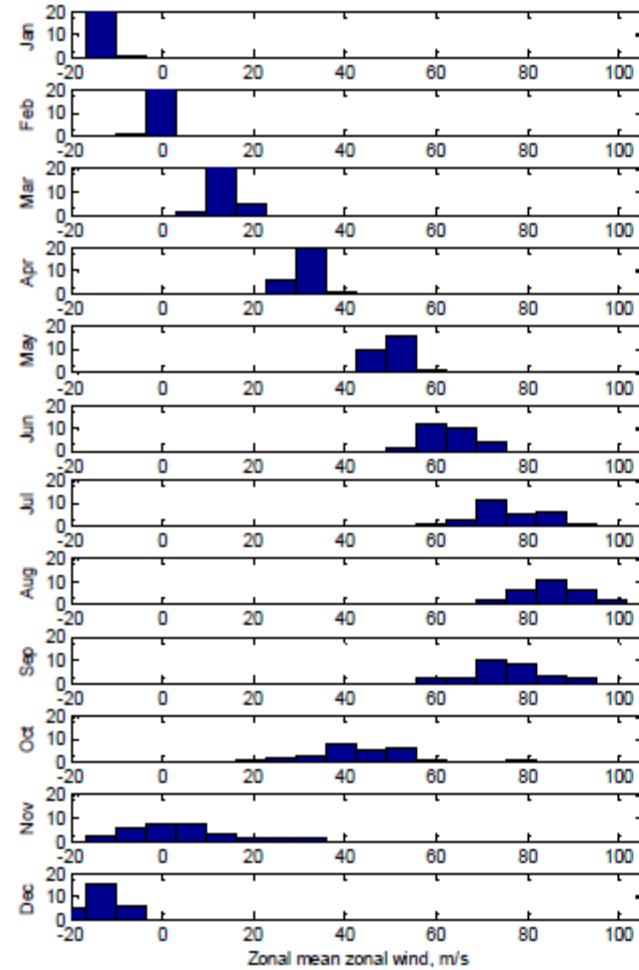


Figure 4. (a) latitudinally averaged EP flux divergence, as a function of height and time for a representative subinterval of the model integration; (b) latitudinally averaged upward EP flux through 200 hPa as a function of time for the same subinterval. The contour interval in (a) is $10^{14} \text{ kg m s}^{-2}$, with negative values (convergence) shaded and darker tones corresponding to larger negative values. Units in (b) are $10^{19} \text{ kg m}^2 \text{ s}^{-2}$.

Frequency distribution of monthly mean zonal winds at 60 deg ERA40 + Interim

S Hem

N Hem



winter
solstice

SSW frequency (/yr)

0.033

0.61

*Sheshadri et al. [2015]
[also Labitztke, Taguchi & Yoden]*

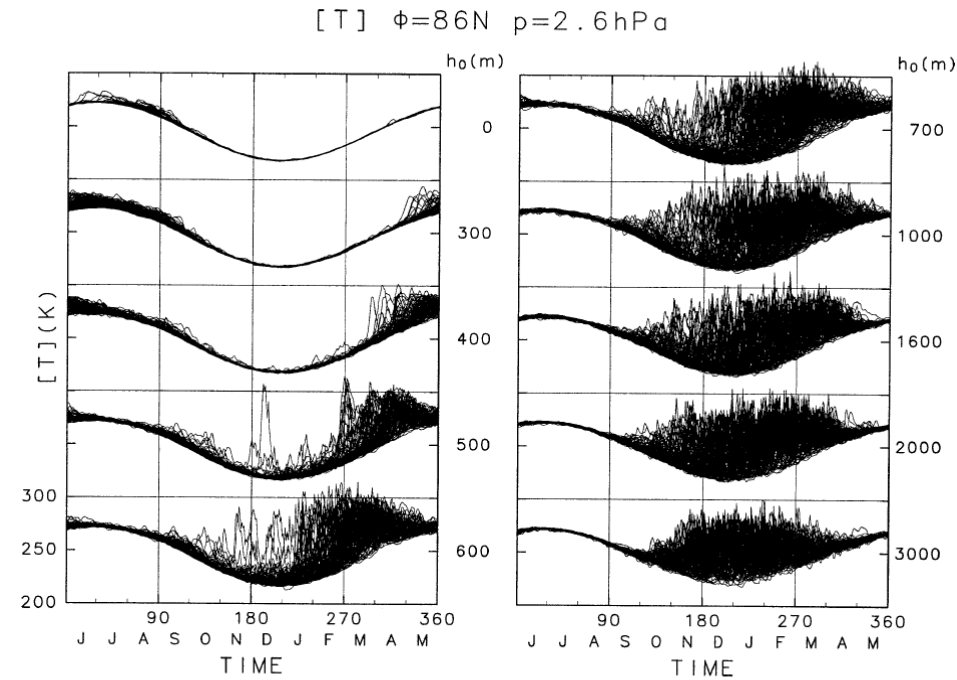


FIG. 5. Daily variations of $[T]$ (K) at $\phi = 86^\circ\text{N}$ and $p = 2.6\text{ hPa}$ for the 100 yr in each run.

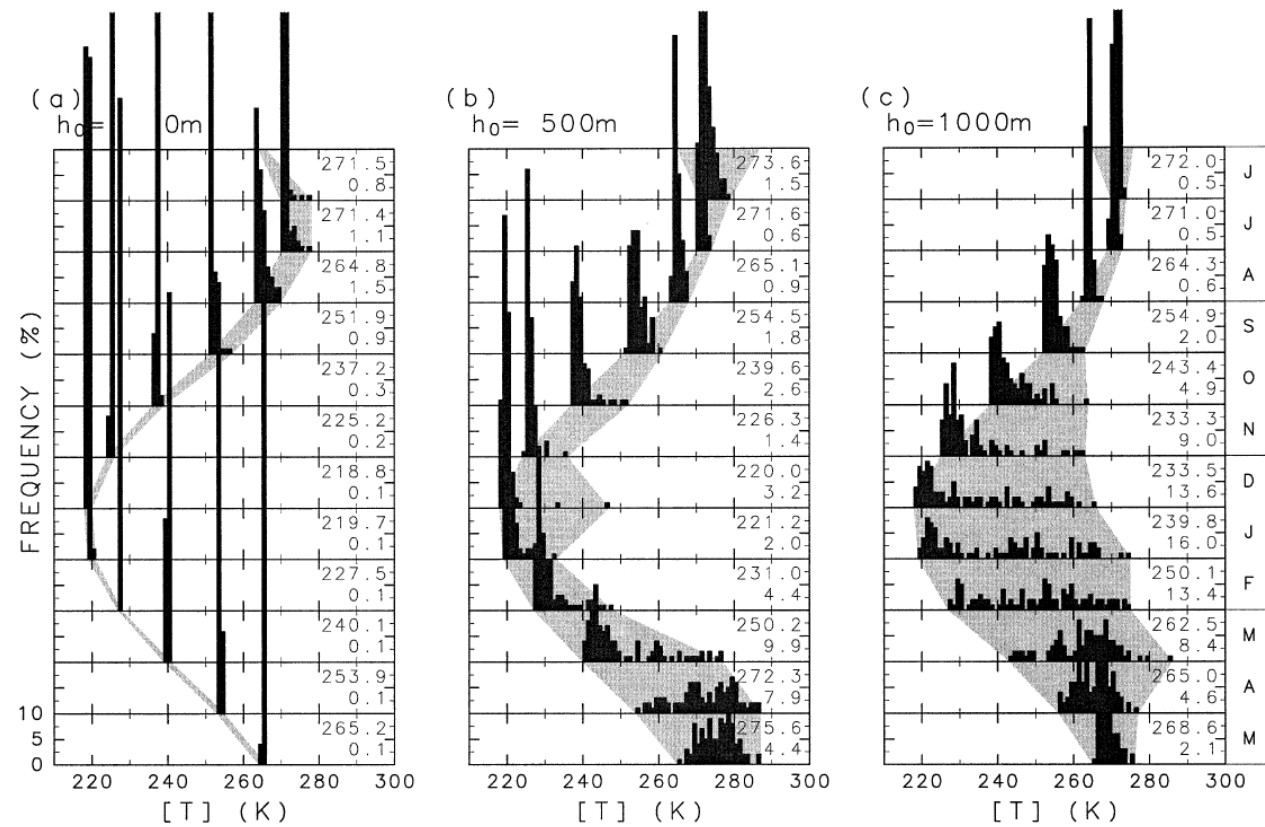
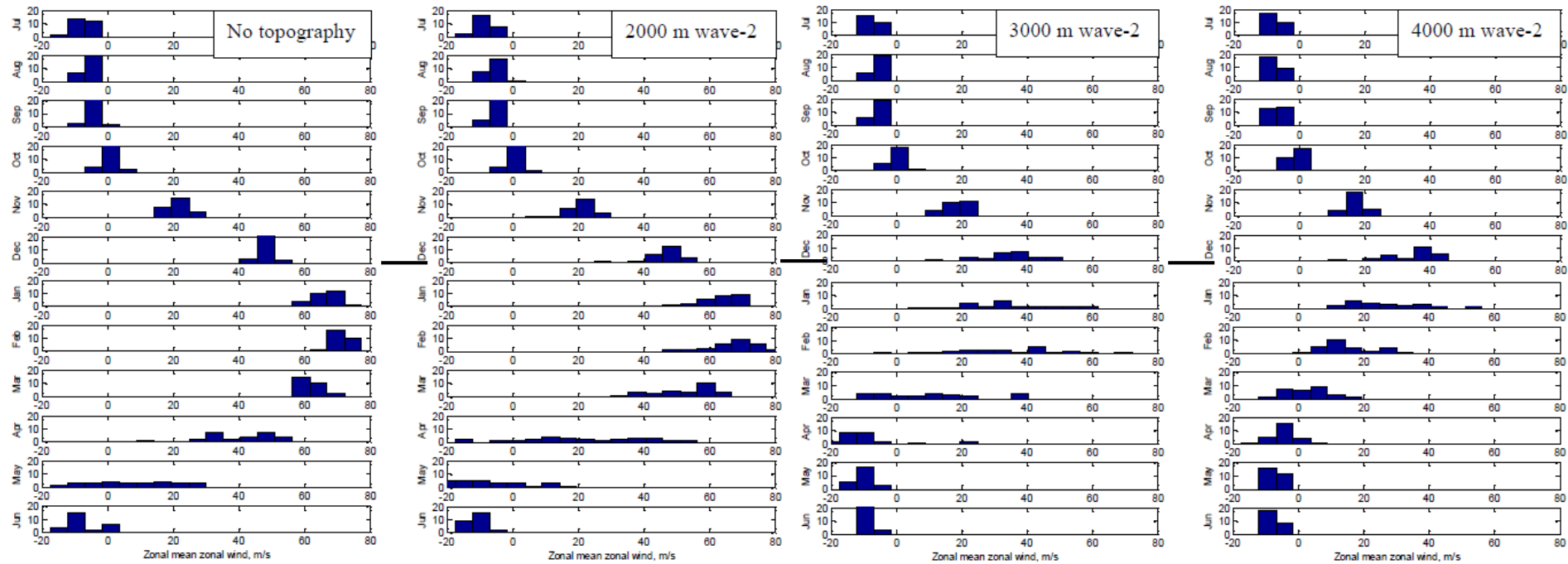


FIG. 6. Frequency distributions of monthly mean $[T]$ at $\phi = 86^\circ\text{N}$ and $p = 2.6\text{ hPa}$ in three runs: (a) $h_0 = 0\text{ m}$, (b) 500 m , and (c) 1000 m . Averages and standard deviations for the 100-yr data are written on the right-hand side of each month (upper and lower numbers, respectively).

Frequency distribution of monthly mean zonal winds at 60 deg Model N Hem with m=2 topography



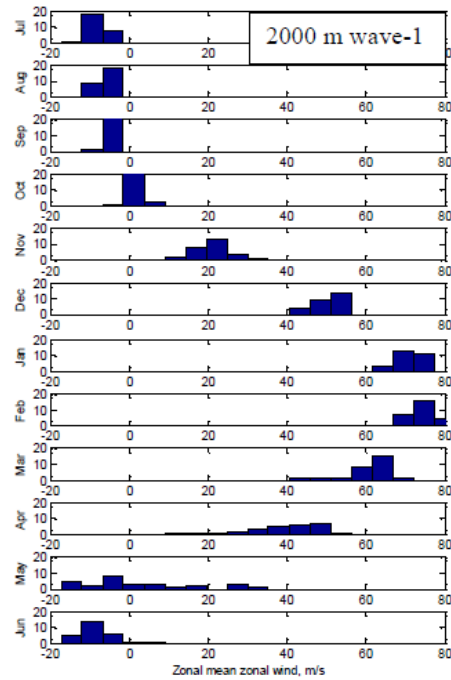
0

0.17

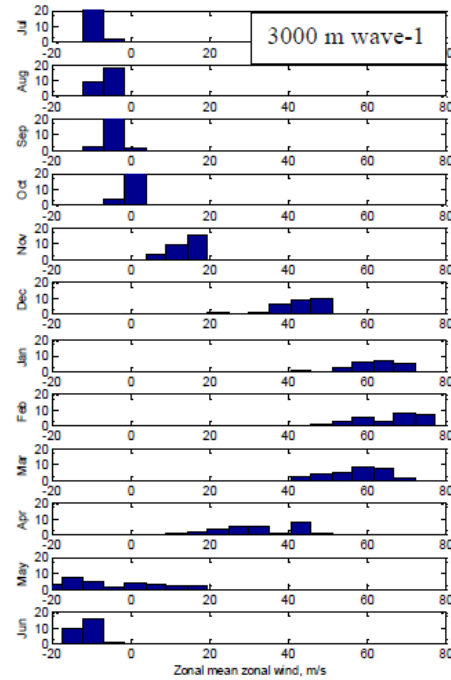
0.20

0.62

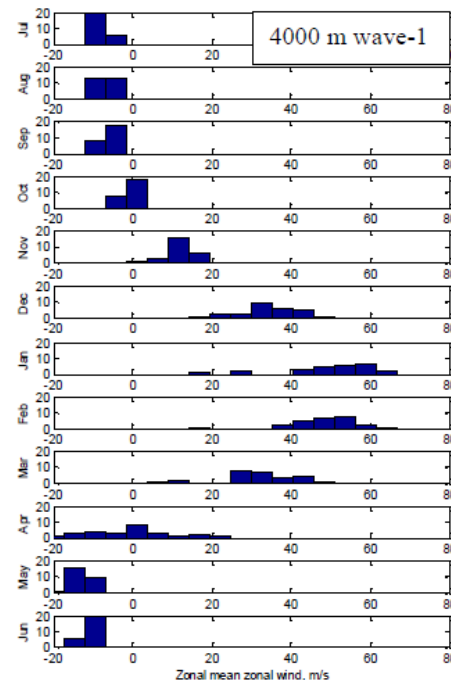
Frequency distribution of monthly mean zonal winds at 60 deg Model N Hem with m=1 topography



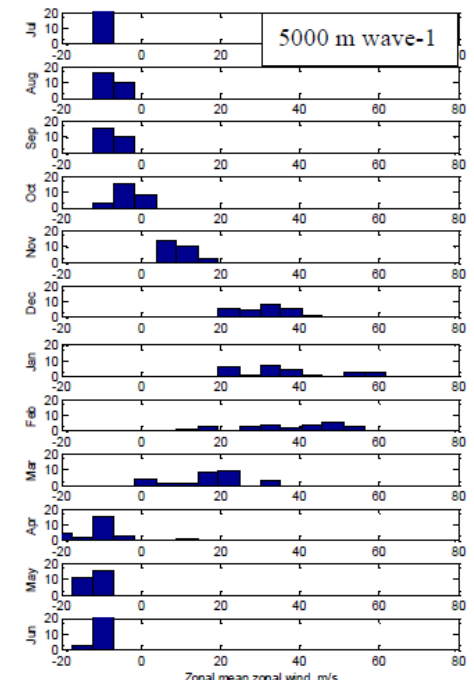
0



0



0.033



0.10

Conclusions (part 1)

- Simplified models (1-D and 3-D) permit experimentation that would be difficult (or less clean) in a full GCM
- Stratospheric variability is not just a response to tropospheric variability, but is at least in part a manifestation of internal dynamical variability
- Both severely truncated (1-D) models and SGCMs exhibit regime behavior, depending on the strength of tropospheric wave forcing
- SGCMs can reproduce the key characteristics of stratospheric variability, its seasonal behavior, and interhemispheric differences, given the right choice of tropospheric forcing

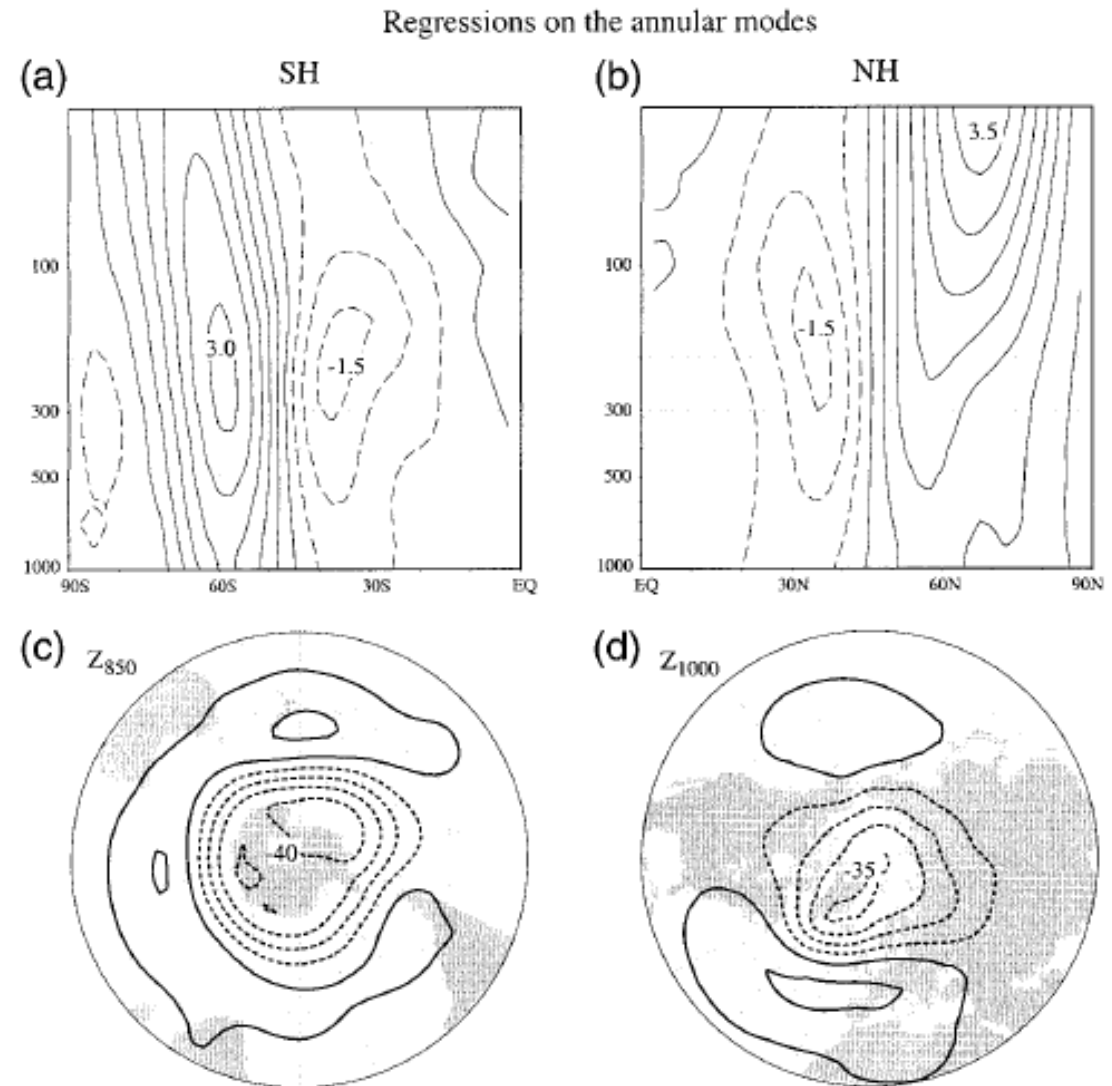
Stratosphere



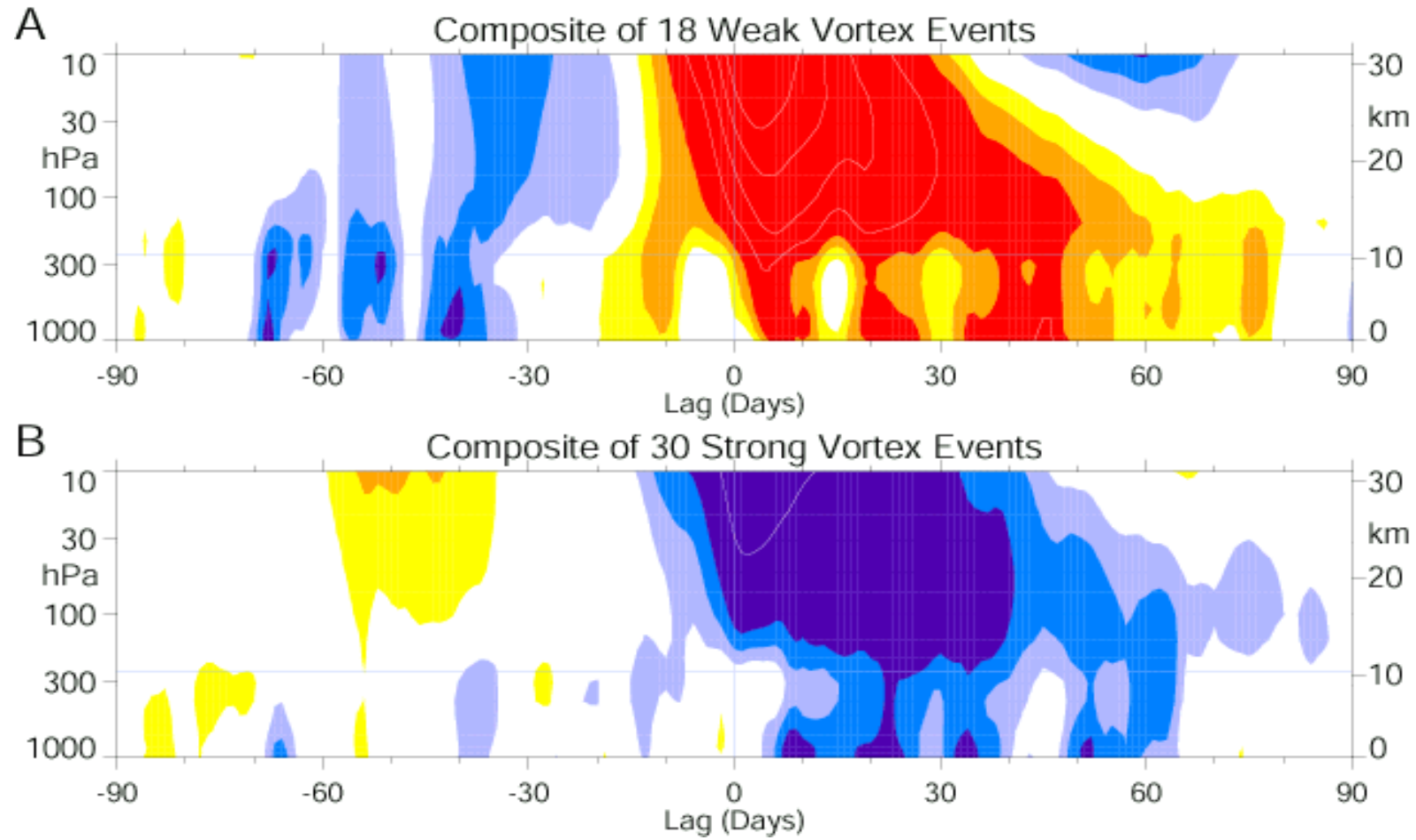
Troposphere

[Thompson and Wallace, 2000]: Annular Modes

- Leading patterns of variability in extratropics of each hemisphere
- Strongest in winter but visible year-round in troposphere; present in “active seasons” in stratosphere



Baldwin & Dunkerton [2001]: Downward migration of the Northern Annular Mode



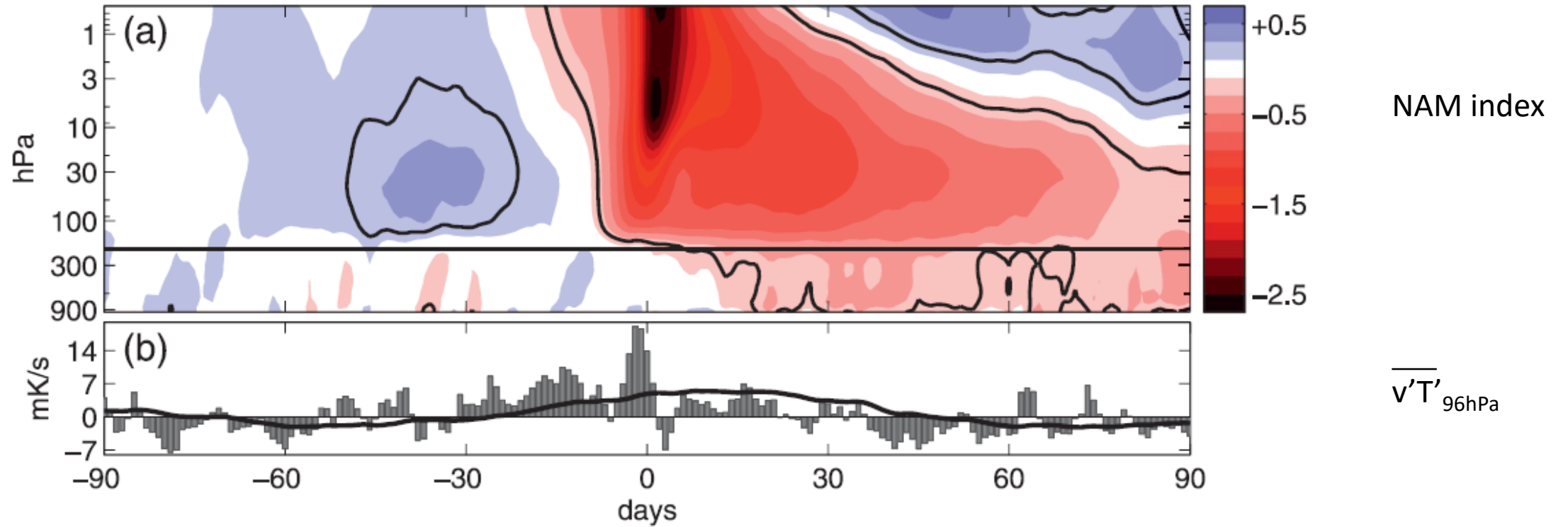


FIG. 8. (a) Composite of the annular mode index as a function of pressure and lag, based on 83 stratospheric sudden warming events determined by the day that the NAM index at 10 hPa drops below -2 standard deviations. Black contours mark areas significantly different from zero with 95% confidence. (b) Composite of \mathcal{H} , the 20° – 90° average meridional heat flux at 96 hPa, as defined in (2), for the same events: \mathcal{H} is proportional to the upward flux of wave activity into the vortex. The solid line denotes the mean of \mathcal{H} over the 40 previous days.

FIG. 3. January mean 1000 mb geopotential height difference (westerly category minus easterly category). Units: geopotential meters.

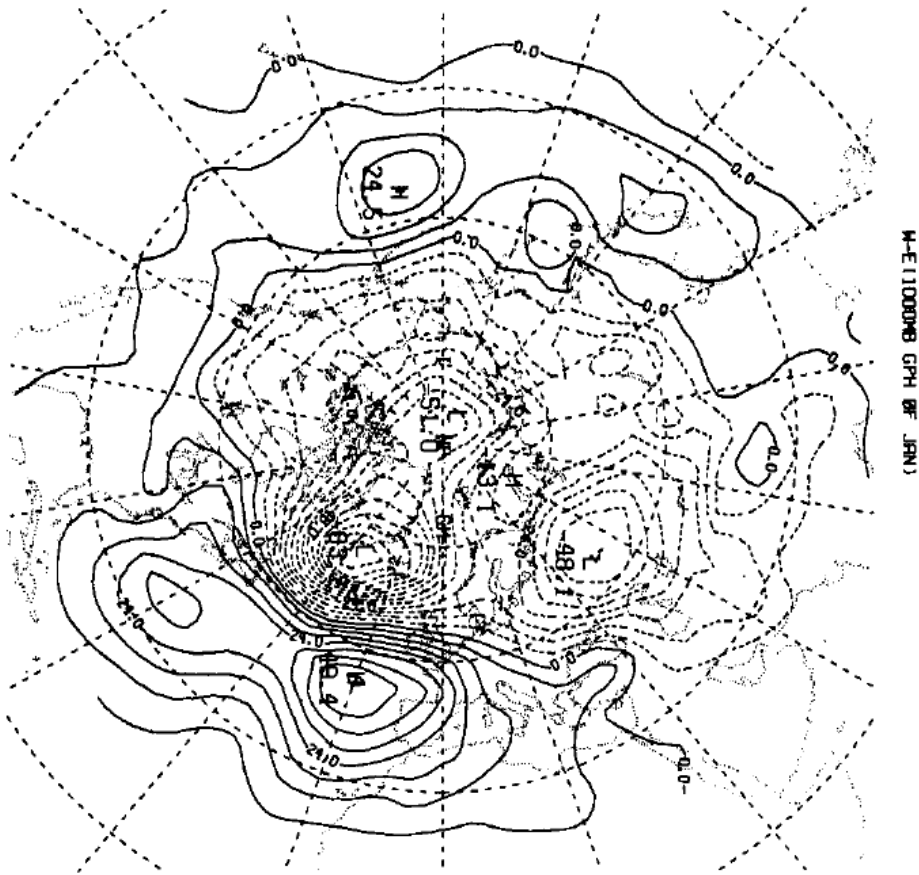


FIG. 3. The ensemble averages of the 500 mb geopotential height field for CS (top), DS (middle) and the difference DS minus CS, (bottom) on a polar stereographic projection with 20°N as the outer boundary. Contour interval is 100 m for upper plots and 50 m for the difference; labels are in decameters. The 5% confidence region is shaded on the difference map.

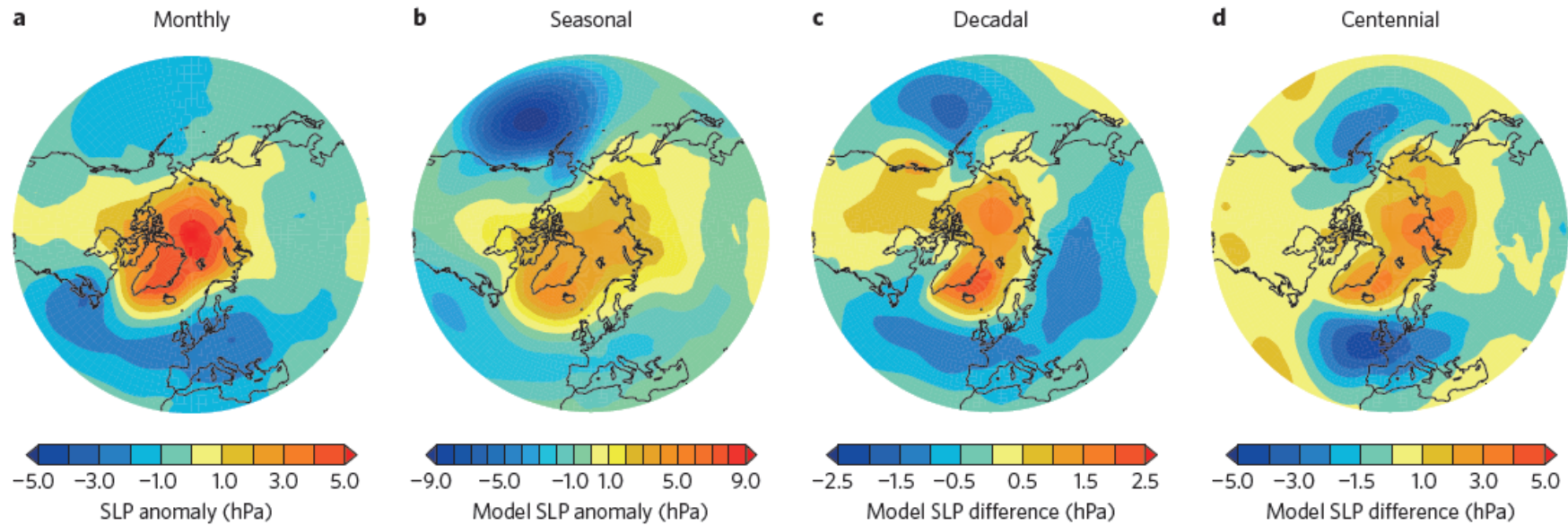


Figure 2 | Northern Hemisphere stratosphere-troposphere coupling across timescales. **a**, Average anomalous sea-level pressure (SLP) in the month after a SSW for 1958–2002 reanalysis. **b**, Composite modelled January–March SLP anomaly for El Niño years with SSWs. **c**, Modelled difference in winter SLP for solar minimum minus solar maximum. **d**, Difference in the projected change in December–February SLP due to a quadrupling of CO₂ in model versions with and without a well-resolved stratosphere. Note the different colour scales. Figure adapted with permission from: **a**, Fig. 12b, ref. 22, © American Meteorological Society; **b**, Fig. 5a, ref. 25, © Macmillan Publishers Ltd; **c**, Fig. 1a, ref. 28, © Macmillan Publishers Ltd; **d**, Fig. 2b, ref. 18, Springer.

[Kidston et al., *Nature Geoscience*, 2015]

Regimes:

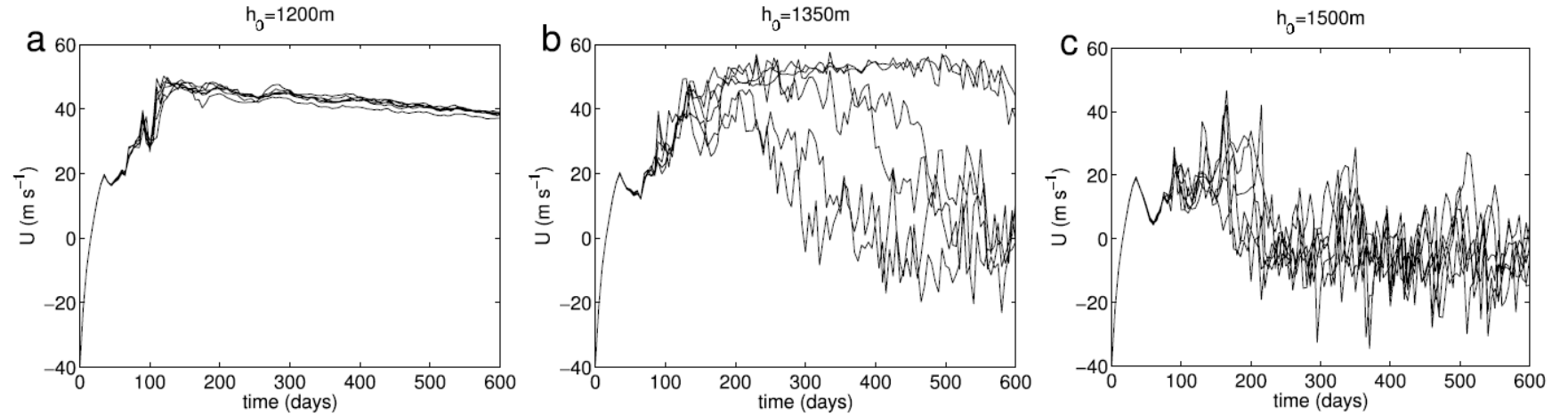


Figure 11. Evolution of velocity U at 58°N and 50 km for (a) cool ($h_0 = 1200$ m), (b) intermediate ($h_0 = 1350$ m), and (c) warm ($h_0 = 1500$ m) regimes. Same as Figure 7 but for the troposphere-stratosphere version of the 3-D model.

Response to high altitude
(35km, 45km) perturbations:

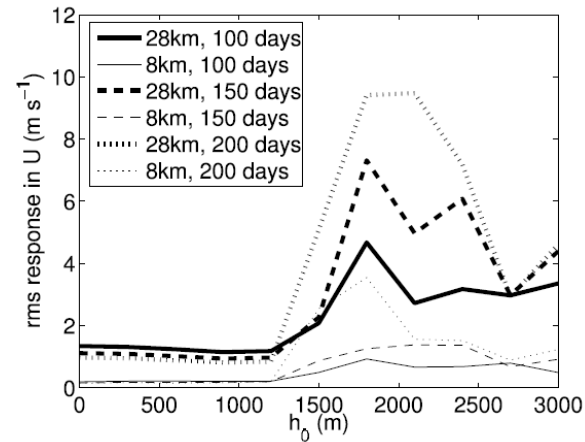


Figure 13. Root-mean-square response in U at 50°N and $z = 28$ km (bold lines) and 8 km (light lines) averaged over the 100 days (solid lines), 150 days (dashed lines), and 200 days (dotted lines) following the perturbation. Same as Figure 10 but for the troposphere-stratosphere version of the 3-D model.

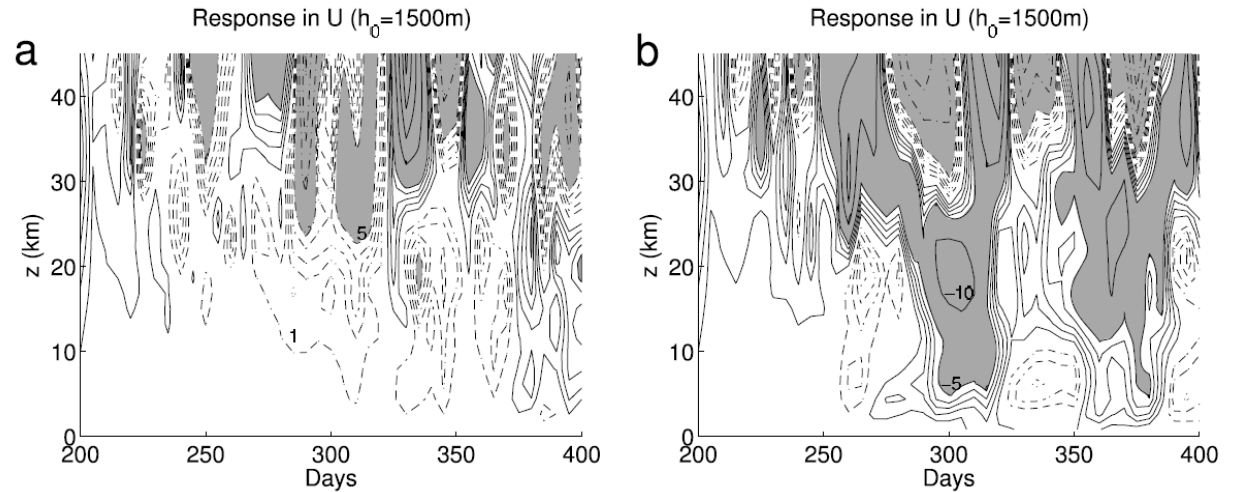


Figure 14. Vertical structure of the response in U for two of the ensemble members in the $h_0 = 1500$ m run of the troposphere-stratosphere version of the 3-D model. Same as Figure 9; notice the different signs, magnitudes, and timings of the response. Contours are as in Figure 9.

Linear stochastic model:
 Principal oscillation patterns (POPs)
 / Empirical normal modes (ENMs)
 [von Storch; Penland]

$$x_t + Ax = f$$

$$X = U\Sigma V^T; \bar{C}_\tau = V_\tau^T V = W\Gamma_\tau W^{-1}$$

$$A = Z\Lambda Z^{-1}; Z = U\Sigma W; \Lambda = \tau^{-1} \ln \Gamma_\tau$$

POPs

free modes:

$$x(\varphi, p, t) = \sum_m Z_m(\varphi, p) e^{\lambda_m t}$$

Climate problem
 (response to steady forcing):

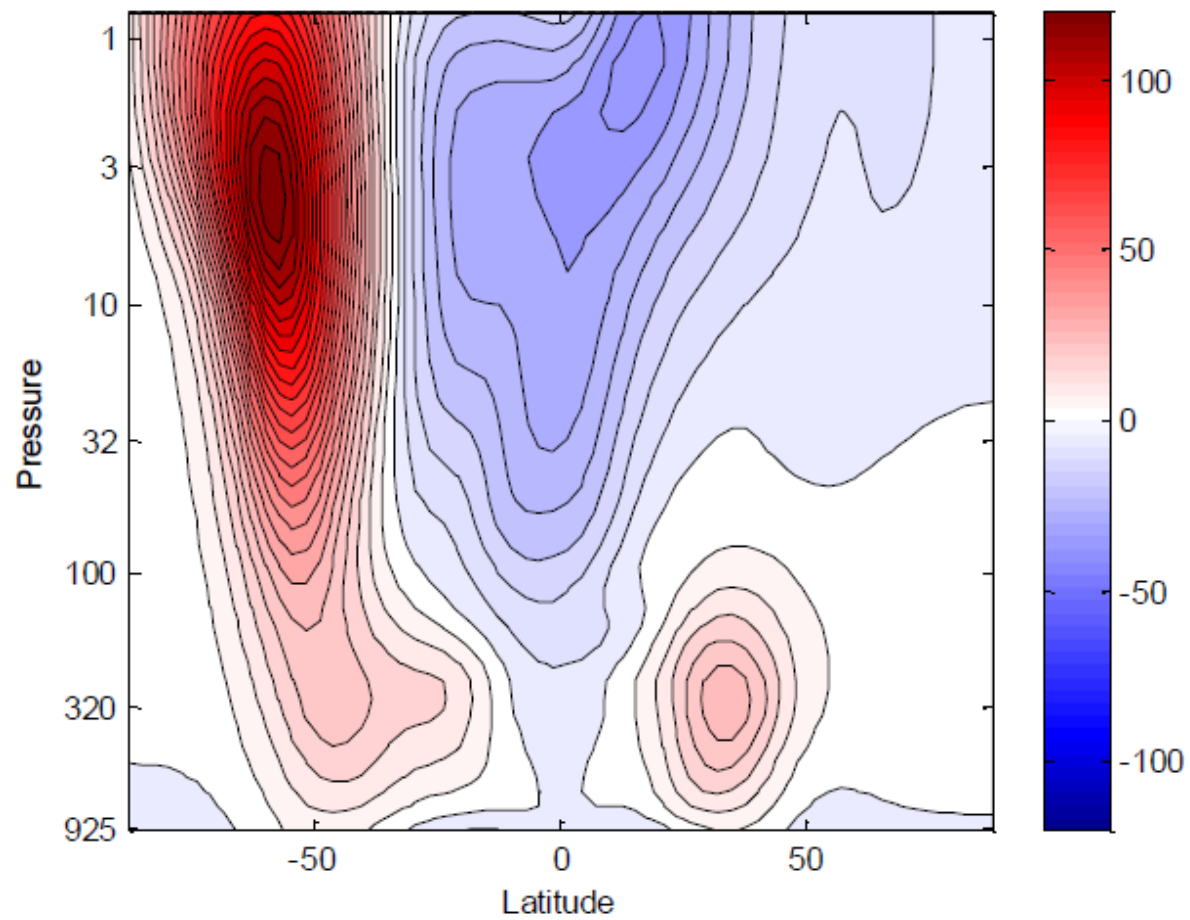
$$x = A^{-1}f$$

$$x(\varphi, p) = \sum_m \lambda_m^{-1} Z_m(\varphi, p) [(Z^{-1})_m \cdot f]$$

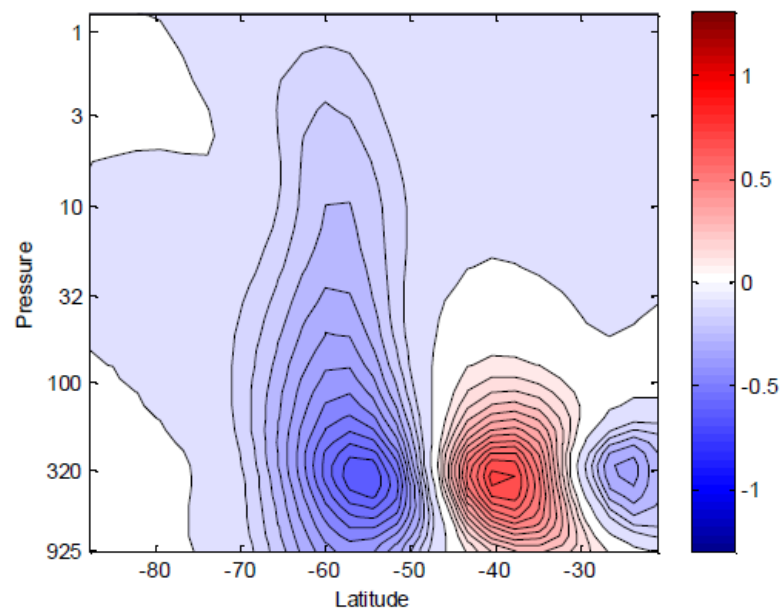
If PCs are independent (zero cross-correlation at all lags) then $Z \Leftrightarrow U$ and

$$\text{Response in } n^{\text{th}} \text{ mode} = \frac{\text{projection of forcing onto mode}}{\text{time scale of mode}}$$

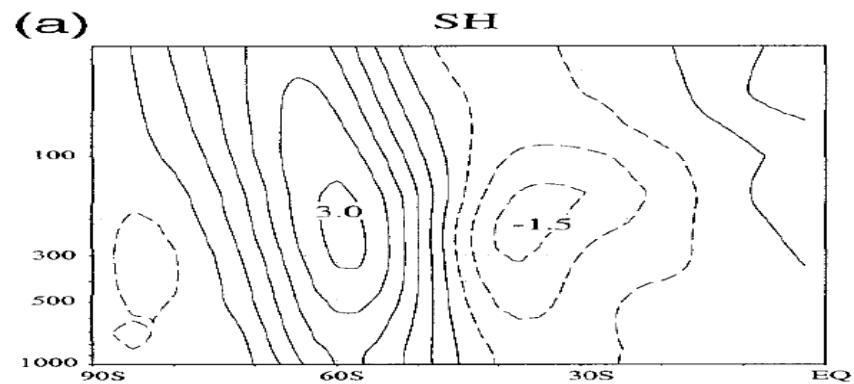
SGCM, no stationary wave forcing,
perpetual southern winter
[Sheshadri & Plumb, 2016]



37% of variance, $\tau=19$ days

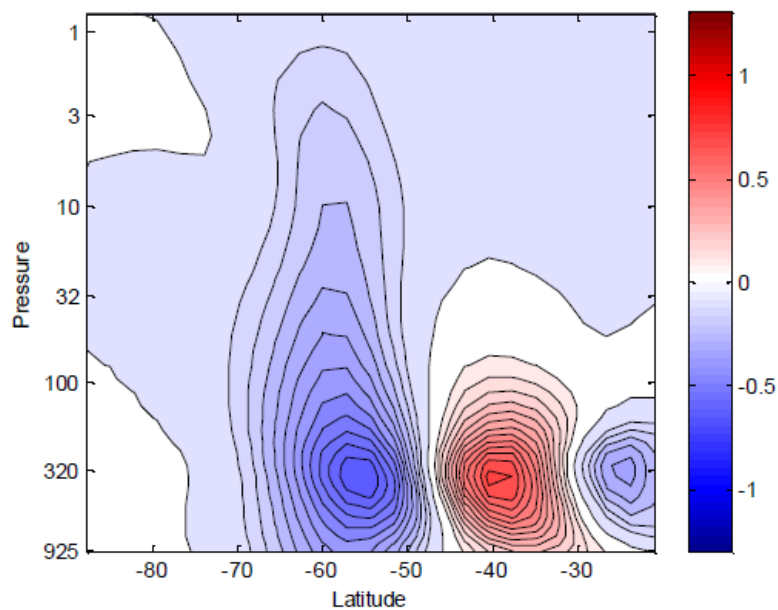


SGCM: Sheshadri & Plumb [2016]

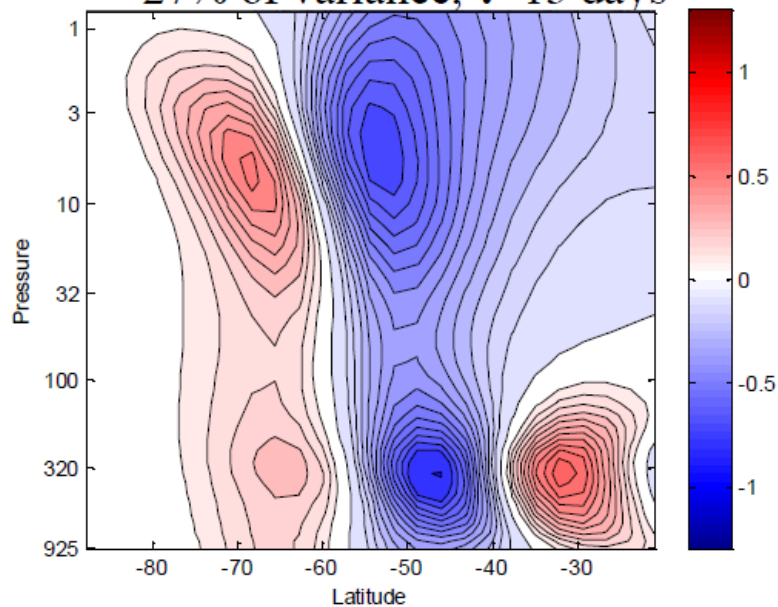


Obs S Hem: Thompson & Wallace [2000]

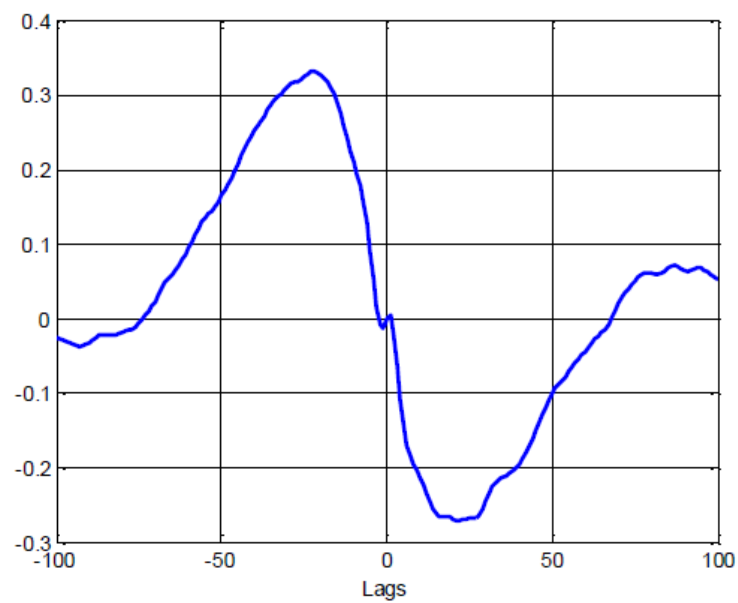
37% of variance, $\tau=19$ days



27% of variance, $\tau=13$ days



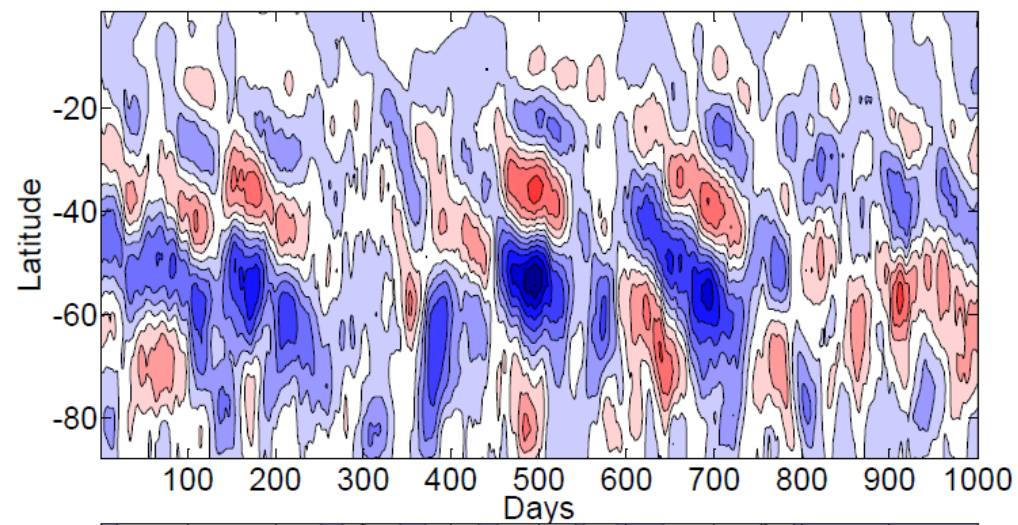
cross-correlation



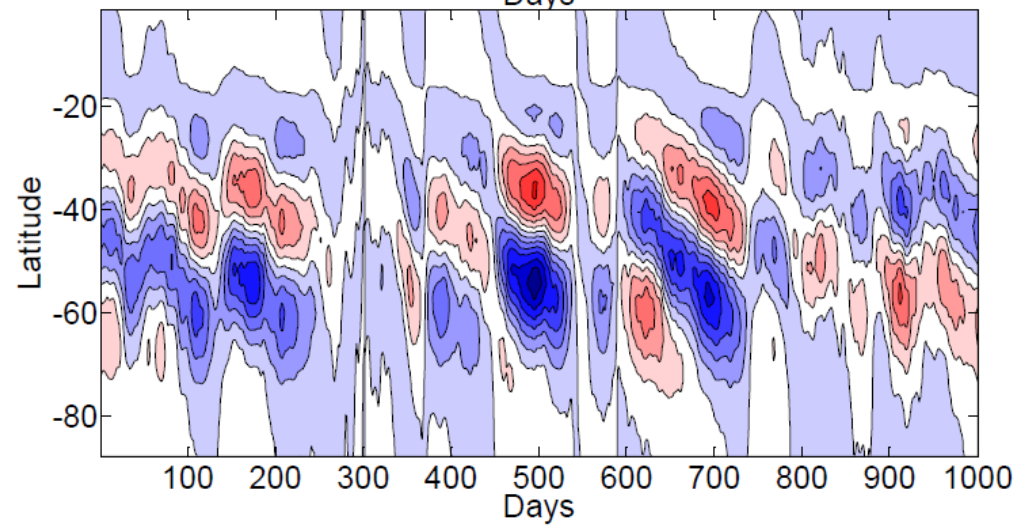
Sheshadri & Plumb [2016]
[also Lorenz & Hartmann, 2001; Son & Lee 2006;
Sparrow et al., 2009]

Anomaly propagation in SGCM

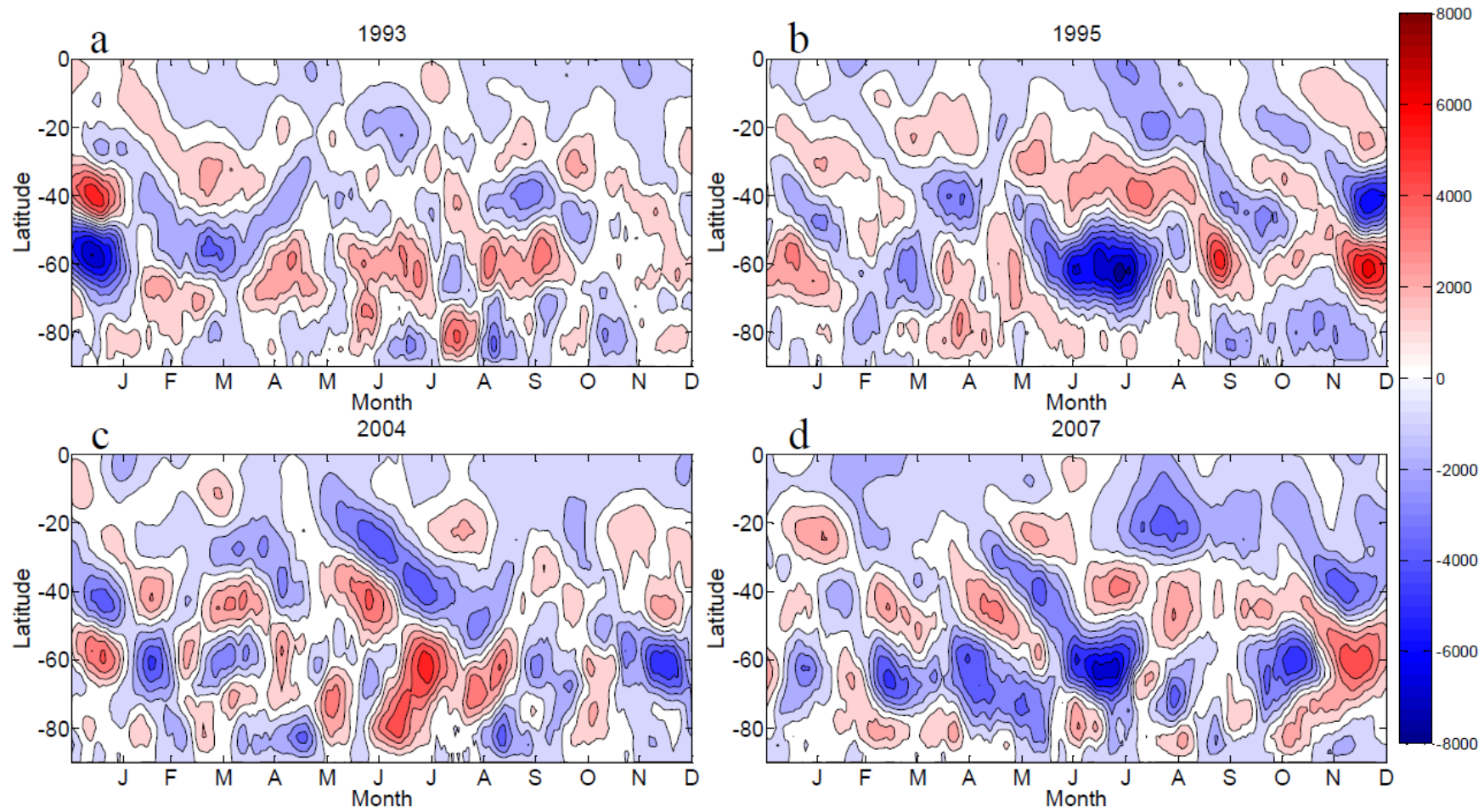
$[\bar{u}](\varphi, t)$



Reconstructed
from EOFs 1+2



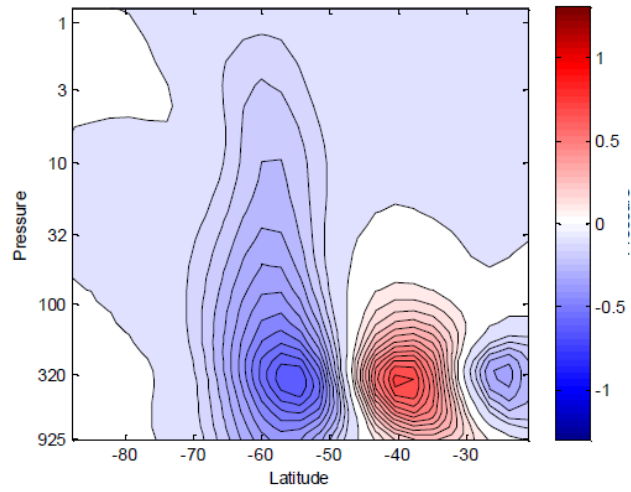
Anomaly propagation in ERAi data



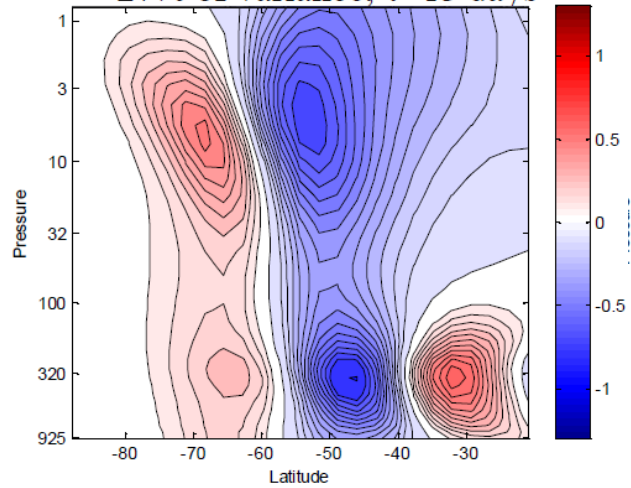
Sheshadri & Plumb [2016] ; *cf.* Feldstein [1998]

EOFs and POPs – SGCM, no stationary wave forcing, perpetual southern winter [Sheshadri]

37% of variance, $\tau=19$ days



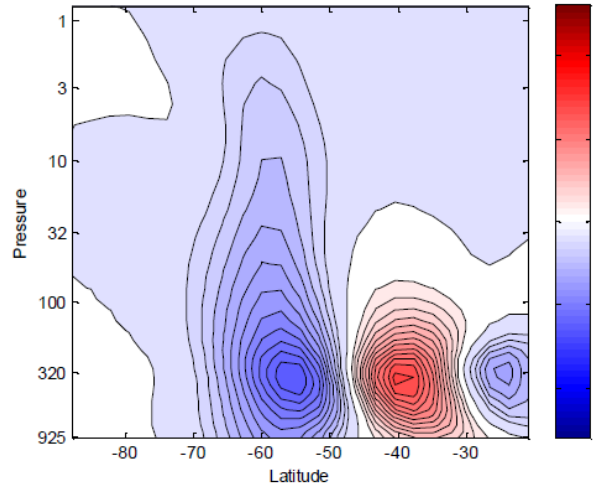
27% of variance, $\tau=13$ days



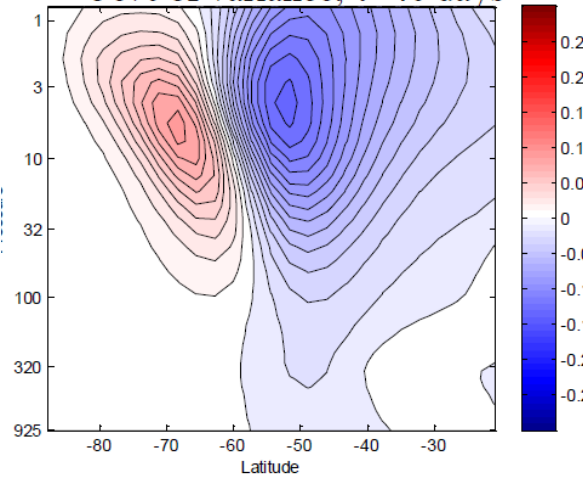
mass-weighted EOFs 1,2

EOFs and POPs – SGCM, no stationary wave forcing, perpetual southern winter [Sheshadri]

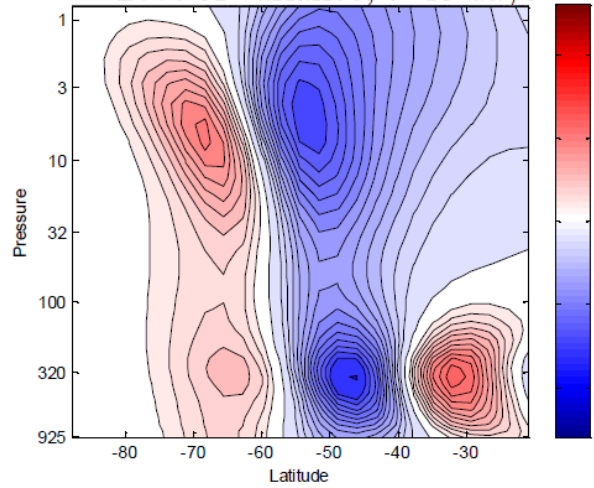
37% of variance, $\tau=19$ days



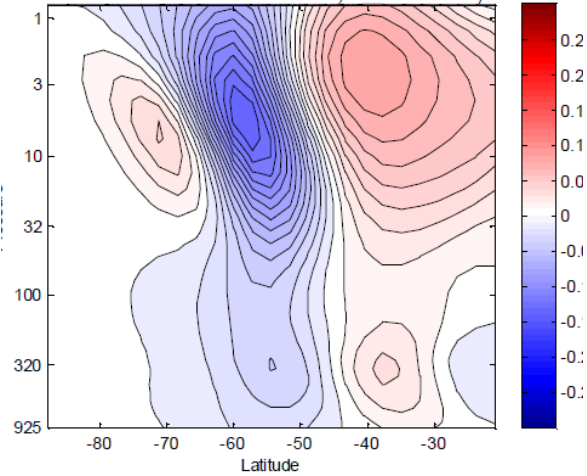
56% of variance, $\tau=40$ days



27% of variance, $\tau=13$ days



12% of variance, $\tau=17$ days

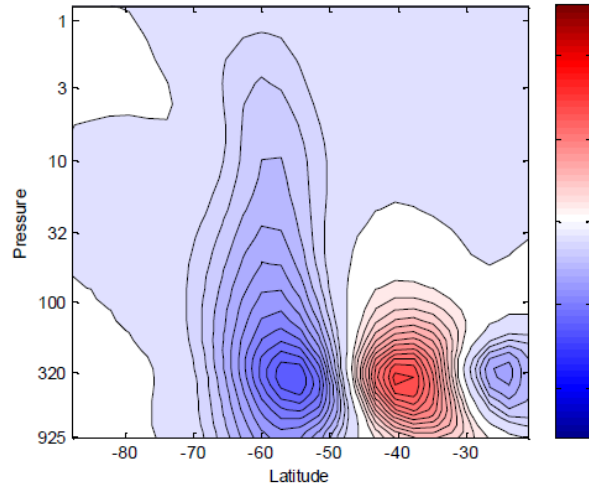


mass-weighted EOFs 1,2

volume-weighted EOFs 1,2

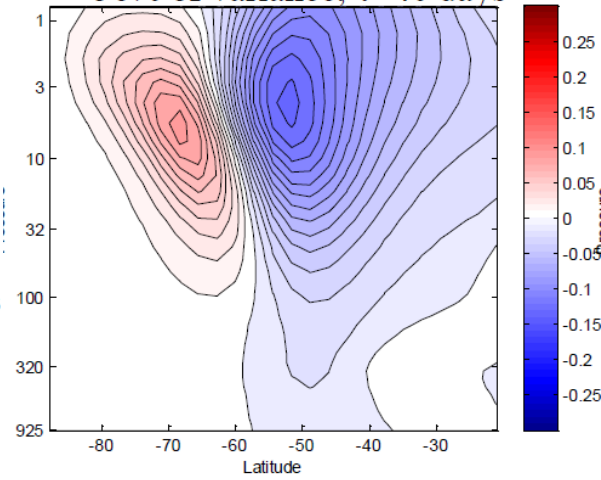
EOFs and POPs – SGCM, no stationary wave forcing, perpetual southern winter [Sheshadri]

37% of variance, $\tau=19$ days



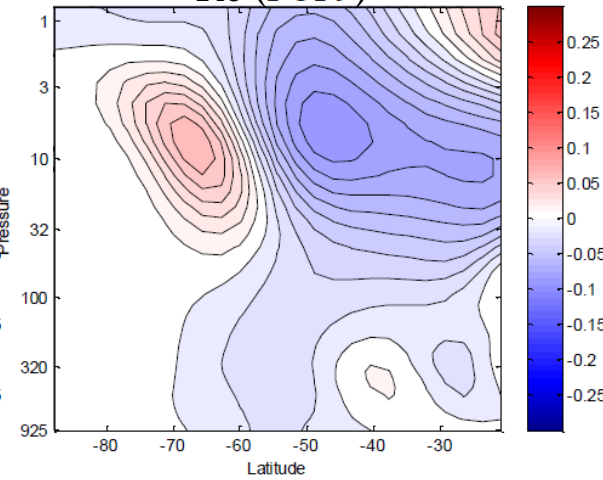
mass-weighted EOFs 1,2

56% of variance, $\tau=40$ days



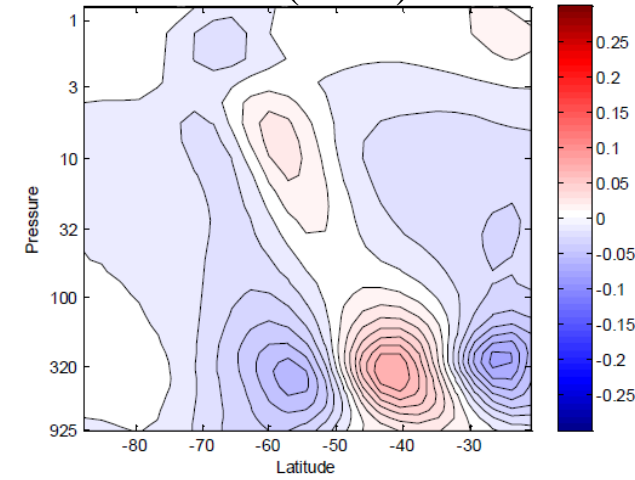
volume-weighted EOFs 1,2

Re (POP9)



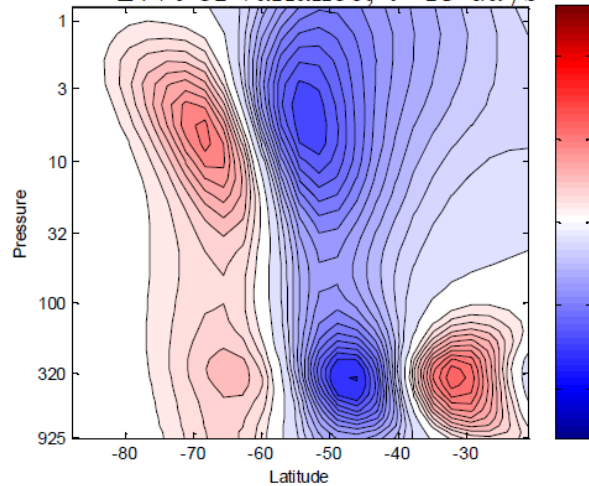
POP 9
decay time 66 d.; period 659 d.

Re (POP35)

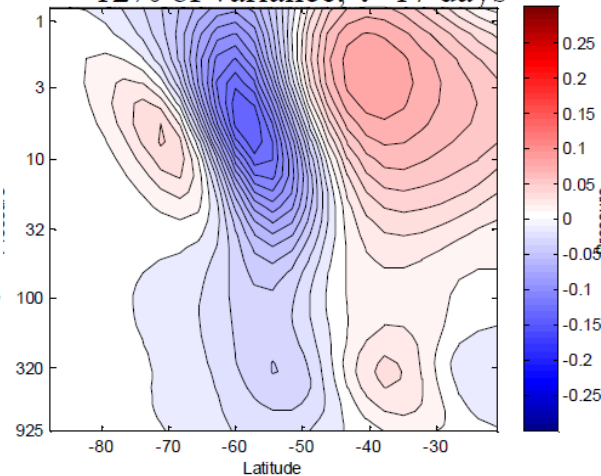


POP35
decay time 39 d.; period 126 d.

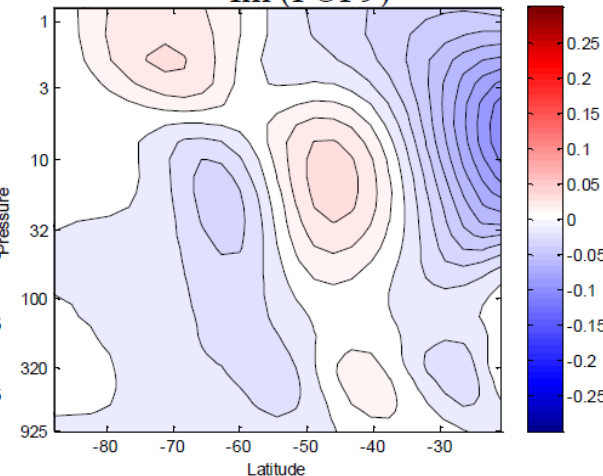
27% of variance, $\tau=13$ days



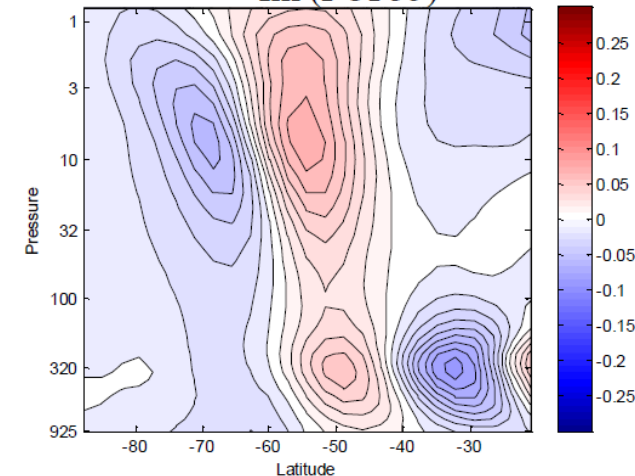
12% of variance, $\tau=17$ days



Im (POP9)



Im (POP35)

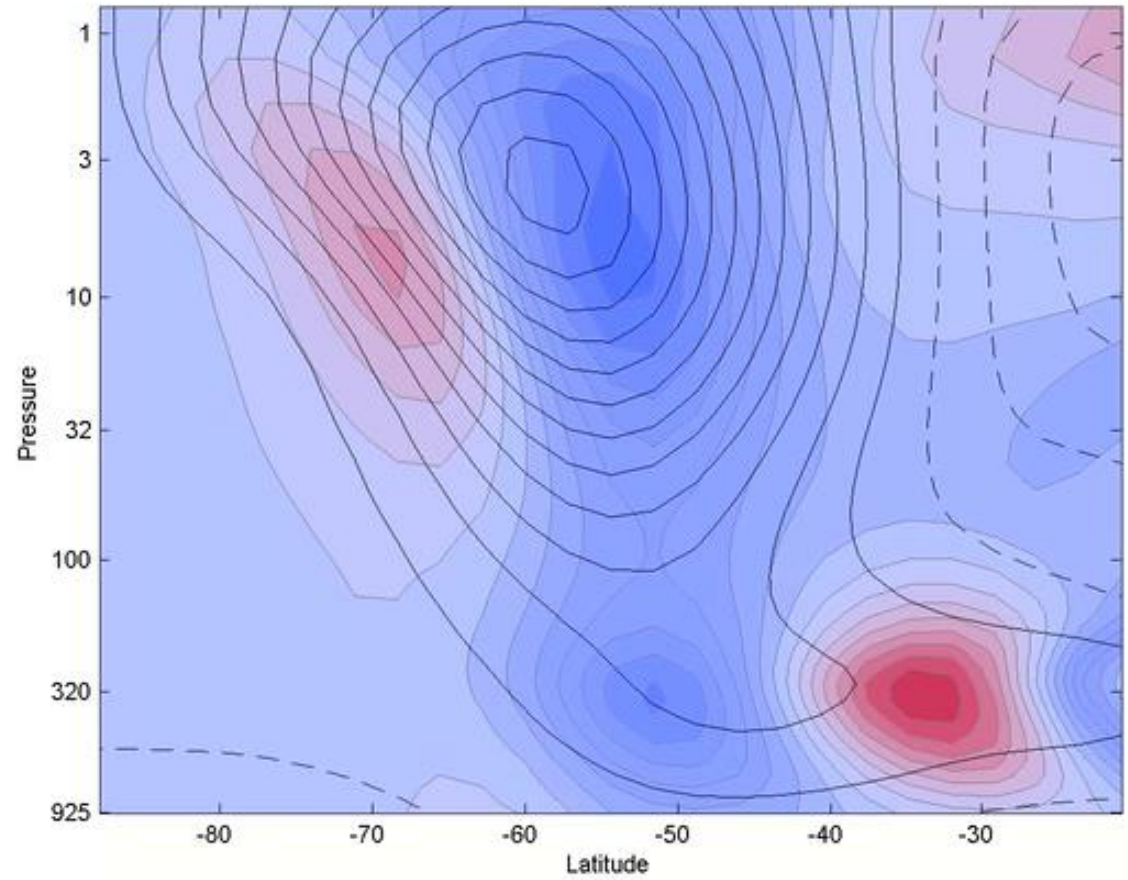


Evolution of POP35

$$u = e^{-\lambda_R t} \times [\text{Re}(Z) \cos \lambda_I t + \text{Im}(Z) \sin \lambda_I t]$$

$$\lambda_R^{-1} = 39 \text{ d}$$

$$2\pi\lambda_I^{-1} = 126 \text{ d}$$



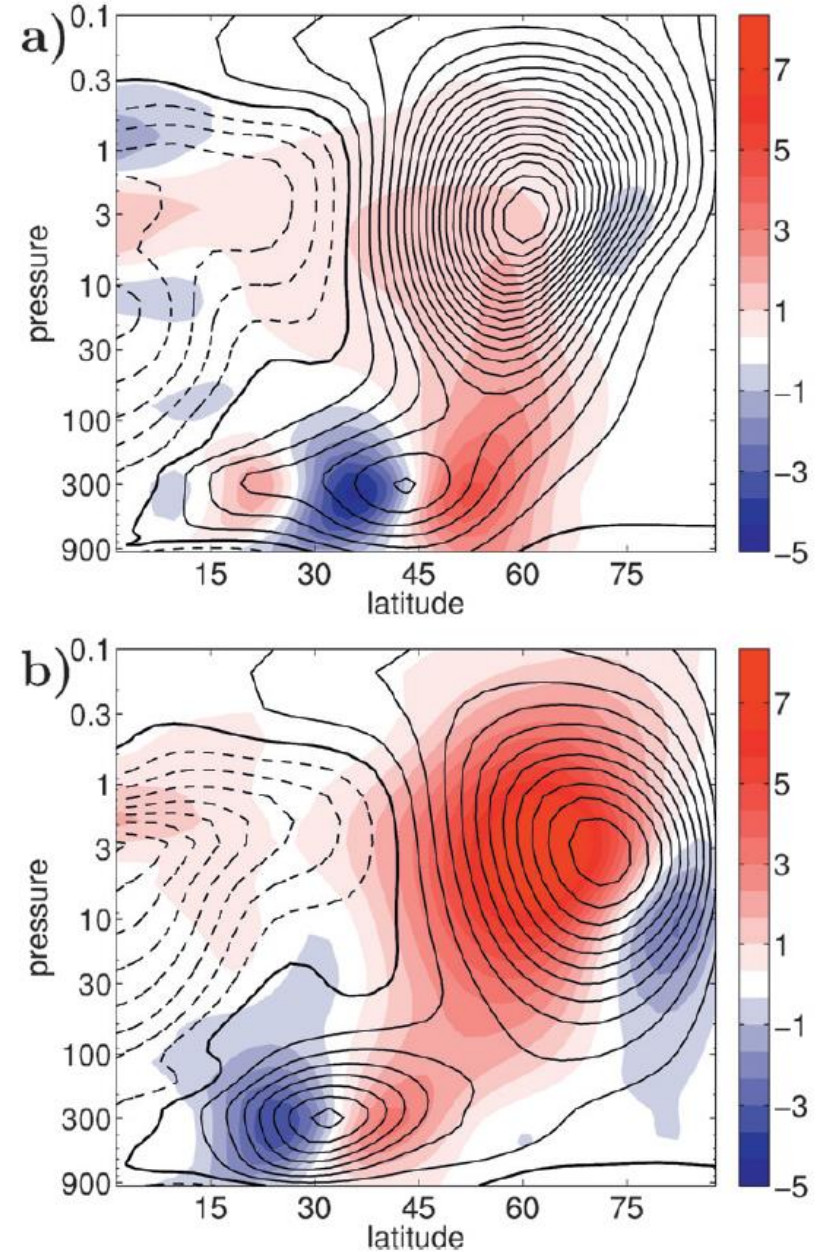
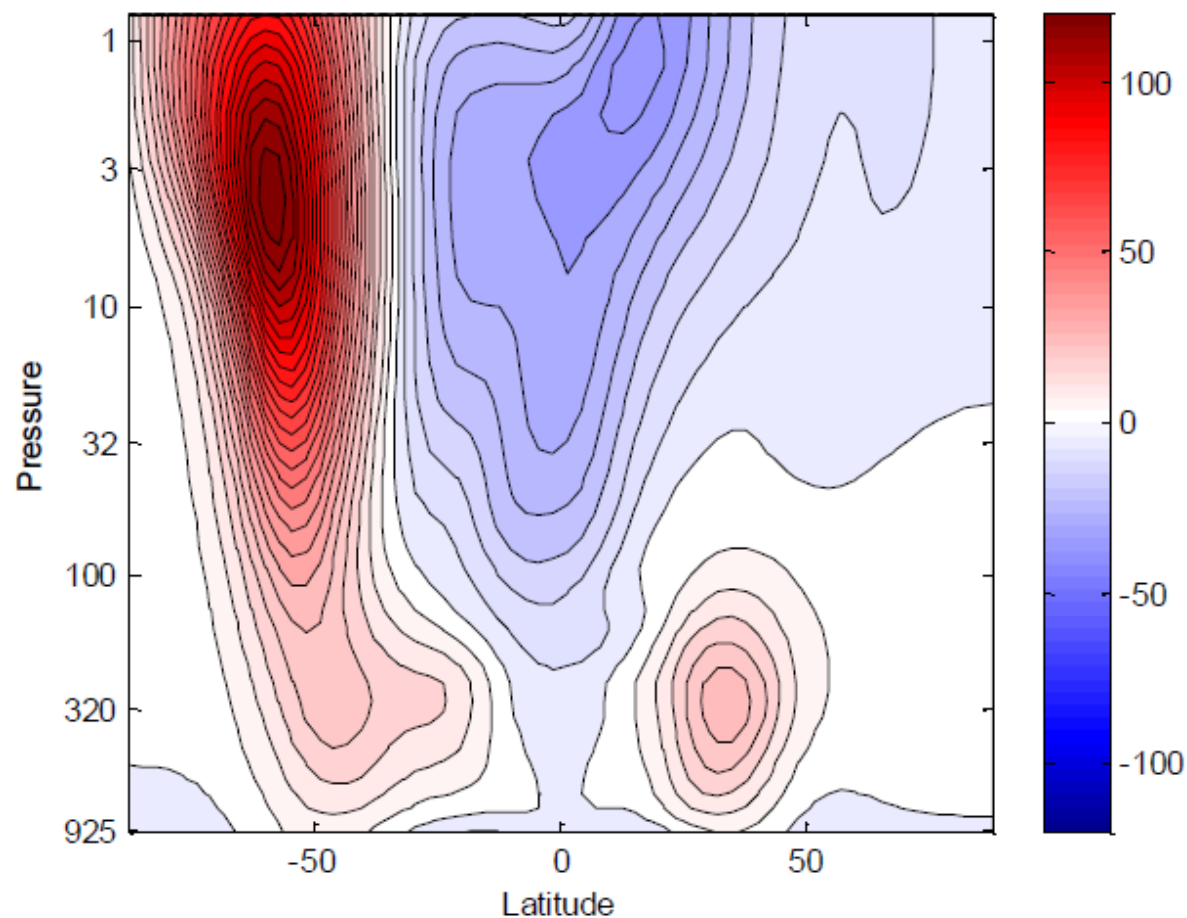


FIG. 7. The annular mode as a function of pressure and height for the model (a) without topography (integration 5) and (b) with wavenumber $m = 2$ topography of amplitude $h_0 = 3000$ m (integration 9). The same strong stratospheric vortex is forced in both cases with $\gamma = 4 \text{ K km}^{-1}$. Contours mark the climatological zonal winds (contour interval 5 m s^{-1} , negative contours dashed, the zero contour in bold) and the color shading denotes the annular mode EOF, with units of meters per second corresponding to a positive one standard deviation anomaly. The two-dimensional annular mode is defined as the first EOF of the pressure and area weighted zonal-average zonal winds from the equator to the pole.

SGCM, no stationary wave forcing,
perpetual southern winter
[Sheshadri & Plumb, 2016]

Imposed forcings in troposphere are
symmetric about the equator!



Conclusions (part 2)

- Reality of tropospheric impacts of stratospheric anomalies is now well established, by model experiments (simplified models and GCMs)
- Mechanism of coupling is still not clear (mean circulation vs. waves)
- Regime behavior in 1-D and 3-D models (N vs S Hem behavior in GCMs and observations consistent with this)
- Suggestions from 1-D models and SGCMs that significant downward influence occurs only in active regimes with large stratospheric variability